A STUDY OF THE BICONICAL ANTENNA

Martin Algirdas Plonus

May 1961

Grant NSF - 11286

National Science Foundation
Washington 25, D. C.

TABLE OF CONTENTS

TABLE OF CONTENTS
(Cont'd.)

TABLE OF CONTENTS
(Cont'd.)

ACKNOWLEDGEMENT

The canadidate is indebted to his committee chairman, Professor K. M. Siegel, who brought this problem to his attention and provided guidance and support for this investigation and to the doctoral committee for correcting the manuscript.

He is especially thankful to Dr. R. F. Goodrich of the Radiation Laboratory for many stimulating conversations and for his invaluable criticism, and to Miss Suzanne Dinga, also of the Radiation Laboratory, for programming many tedious calculations on the IBM-704.

The author is grateful to Professor R. C. F. Bartels of the Computing Center for providing the computer time.

The research reported in this thesis was supported by the National Science Foundation under Grant NSG 11286.

LIST OF TABLES

LIST OF ILLUSTRATIONS

LIST OF ILLUSTRATIONS
(for Appendix C)

ABSTRACT

The problem of finding the input impedance to a biconical antenna has presented considerable difficulty. First, the roots of the equation

$$P_{n_i}(\cos\theta_o) - P_{n_i}(-\cos\theta_o) = 0$$

for arbitrary cone angle are difficult to find exactly, and second, the exterior mode coefficients in terms of which the radiated field and the input impedance is expressed are defined by an infinite matrix.

In this study the roots to the above equation are obtained by using asymptotic expressions for the Legendre functions. The theory of the biconical antenna, particularly the process of mode matching, is then examined and several interesting observations are made which lead to two methods, one for thin cones and one for thick cones, for obtaining the exterior mode coefficients. A further investigation reveals that for arbitrary cones a finite set of preferred modes exists which behave similarly to the modes of infinitesimally thin cones. From this a method is developed which approximates each interior mode coefficient by a finite number of exterior modes, called the subset. The terms in this finite subset are then shown to depend on the solution of a finite matrix which is of the same order as the number of terms in the subset. Finally, any exterior mode coefficient is determined from an expression which relates this coefficient to all interior modes. It is important to realize that any desired accuracy in this method of approximation can be realized by including a sufficient number of terms in the finite subset of preferred modes.

The numerical calculations for the input impedance were carried out on the IBM-704. The results for various cone angles and cone length are shown in graphical form. In general, the roughest approximation, one that includes only a single term in the subset, shows good agreement with existing data for biconical antennas.

I

INTRODUCTION

The theory for the biconical antenna has been formulated by S. A. Schelkunoff [1] in 1941. Further contributions have been made by C. H. Papas and R. King [2] in 1948, by P. D. P. Smith [3] in 1948 and by C. T. Tai [4] in 1949. The most recent one is that by L. Robin and A. Pereira-Gomes [5] in 1953.

Schelkunoff's treatment of the biconical antenna can be referred to as a mode analyses, since it bears a striking similarity to that usually employed in transmission line and waveguide theory. The input impedance and the radiated electromagnetic field of the biconical antenna are expressed as a summation of modes, each mode having an unknown coefficient. The unknown coefficients are determined from an infinite set of simultaneous equations. It is this infinite set of equations which has prevented the mode theory from becoming a simple and elegant one. Whenever the input-impedance to a particular biconical antenna was desired, the infinite set was truncated and the unknown mode coefficients were found from the resulting solutions. Since the infinite matrix is quite unmanageable the highest order truncation to date is a three by three matrix [5].

In this study various methods are presented which circumvent the infinite matrix for the mode coefficients and give them explicitly. Some of these methods depend on the cone angle of the biconical antenna; for example for infinitesimally thin cones and for thick cones whose cone angle approaches 90^o, the mode coefficients are known exactly. Such cone angle dependent methods result in the desired simplicity. An asymptotic series for the mode coefficients is also derived which is valid for any cone angle.

Before this present investigation was attempted the theory of the biconical antenna was reviewed. A good account of this theory is given in Schelkunoff [6] . To gain some additional insight the corresponding two-dimensional problem of the biconical antenna — called the bi-wedge — was solved. This is presented in Appendix C of this study.

The method and solution for the biconical antenna are inherently more difficult than the ones for the bi-wedge. The biconical antenna presents a three-dimensional boundary value problem in spherical coordinates, whereas the bi-wedge is a two-dimensional one and can be formulated in cylindrical coordinates. In cylindrical coordinates the angular dependence is given by the sine and cosine functions and the radial dependence by the Bessel functions, whereas in spherical coordinates the angular dependence is given by the Legendre functions and the radial dependence by the spherical Bessel functions. Furthermore the summation index is determined from a trigonometric relationship in cylindrical coordinates, but in spherical coordinates the summation index is given by a solution to an equation whose terms are Legendre functions.

II

SUMMARY OF THE THEORY OF THE BICONICAL ANTENNA

A brief summary of the formulation of the biconical antenna as a boundary value problem will now be given. A detailed derivation appears in [6] and [3]. Figure 1 shows the cross section of the biconical antenna and the notation used.

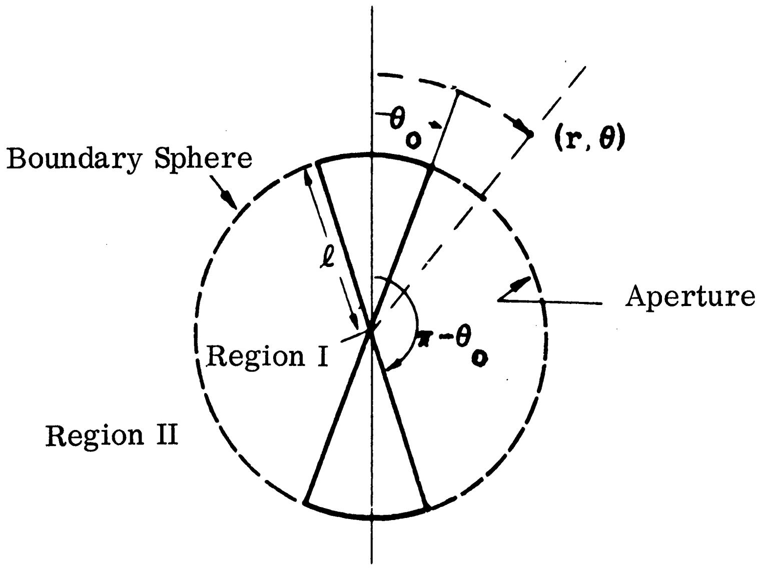

FIGURE 1. CROSS SECTION AND NOTATION OF THE BICONICAL ANTENNA

The biconical antenna is a configuration of a truncated or capped bi-cone, formed by two equal, coaxial and perfectly conducting, solid cones whose apices are infinitely close. The ends of the cones are spherical caps of radius ℓ equal to the generators of the cones. In spherical coordinates this geometry specifies two regions, one with the conducting surfaces of the capped bi-cone, the other the free space surrounding the bi-cone. In each region the field is expanded in an infinite series with unknown coefficients and appropriate functions. The boundary conditions and the continuity of the fields across the regions now help to relate the two coefficients a_{n_i} and b_m of the two regions. The relationship turns out to be an infinite matrix with b_m as the unknowns.

The exterior field is given by E_θ, E_r and H_θ. One of these, E_θ, is

$$E_\theta = \frac{\eta}{i 2\pi r} \sum_{m=1,3}^{\infty} \frac{b_m}{m(m+1)} \frac{\frac{d}{dkr}(kr)^{1/2} H^{(2)}_{m+1/2}(kr)}{(k\ell)^{1/2} H^{(2)}_{m+1/2}(k\ell)} \frac{d}{d\theta} P_m(\cos\theta). \tag{II-1}$$

Similarly in the interior region the E_θ field is given by

$$E_\theta = \frac{\eta}{i2\pi r} \sum_{i=1,2}^{\infty} \frac{a_{n_i}}{n_i(n_i+1)} \frac{\frac{d}{dkr}(kr)^{1/2} J_{n_i+1/2}(kr)}{(k\ell)^{1/2} J_{n_i+1/2}(k\ell)} \frac{d}{d\theta} L_{n_i}(\theta) \tag{II-2}$$

where

$$L_{n_i}(\theta) = \frac{1}{2}\left(P_{n_i}(\cos\theta) - P_{n_i}(-\cos\theta)\right) \tag{II-3}$$

and

$$\eta = \sqrt{\frac{\mu_o}{\epsilon_o}} = 120\pi \text{ ohms}.$$

Another mode which is related to the source exists in the interior region. This is the dominant mode, corresponding to n = 0. The n_i's are determined from

$$P_{n_i}(\cos\theta_o) - P_{n_i}(-\cos\theta_o) = 0 \tag{II-4}$$

which results when the tangential electric field in the interior region is forced to vanish on the surface of the cone of angle θ_o. This is an important equation in the theory of the biconical antenna and the solution for the characteristic values n_i has caused considerable difficulty. When the cone angle θ_o is small, it can be shown by using asymptotic forms for the Legendre functions with arguments approaching 1 (i.e. $\theta_o \rightarrow 0^o$) that the solutions to the above equations are the odd integers. However, when θ_o gets larger than some small angle these asymptotic forms are no longer valid and a more exact method for the solutions must be found. For the wide angle cones, Smith [3] has plotted a graph for n_i which was constructed by interpolating between the Legendre polynomials. Tai [4] used the Ritz method to get approximations for the first few roots. The most complete approach to this problem was made by Robin and Pereira-Gomes [5]. They used asymptotic forms for the Legendre functions for $\theta > \frac{1}{n}$ when $n \rightarrow \infty$ and LaGrange's formula to expand the above equation and then solve for n_i. Numerical calculations to 3 decimal place accuracy were carried out for the first eight roots and for five conical angles ($\frac{\pi}{12}$, $\frac{\pi}{6}$, $\frac{\pi}{4}$, $\frac{\pi}{3}$, $\frac{5\pi}{12}$). However, this procedure proved to be a complicated one.

Boundary conditions are used now to obtain a relationship between the interior and exterior coefficients a_{n_i} and b_m. Thus,

$$a_{n_i} = (2n_i + 1) \frac{1}{\frac{\partial}{\partial n_i} L_{n_i}(\cos\theta_o)} \sum_{m=1,3}^{\infty} \frac{b_m P_m(\cos\theta_o)}{m(m+1) - n_i(n_i+1)} \tag{II-5}$$

and

$$\frac{b_r}{2r+1}\,\frac{R'_r(k\ell)}{R_r(k\ell)} = -i\,P_r(\cos\theta_o) + \sin\theta_o\, r(r+1)\,P_r(\cos\theta_o)$$

$$\sum_{i=1,2}^{\infty} \frac{a_{n_i}}{n_i(n_i+1)}\,\frac{1}{n_i(n_i+1) - r(r+1)}\,\frac{S'_{n_i}(k\ell)}{S_{n_i}(k\ell)}\,\frac{\partial}{\partial\theta_o} L_{n_i}(\cos\theta_o)$$

(II-6)

where

$$R'_r(k\ell) = \frac{d}{dk\ell} R_r(k\ell) \tag{II-7}$$

$$R_r(k\ell) = (k\ell)^{1/2} H^{(2)}_{r+1/2}(k\ell) \tag{II-8}$$

$$S_{n_i}(k\ell) = (k\ell)^{1/2} J_{n_i+1/2}(k\ell)\,. \tag{II-9}$$

The extension of the caps of the bi-cone defines a fictitious mathematical boundary. When the interior and exterior fields are forced to be continuous at this boundary the following matrix relationship for b_m results:

$$P_r(\cos\theta_o) + \frac{1}{2r+1}\,\frac{R'_r(k\ell)}{R_r(k\ell)}\,b_r = \sin\theta_o\, P_r(\cos\theta_o)\, r(r+1) \sum_{m=1,3}^{\infty} b_m P_m(\cos\theta_o)\,\cdot$$

$$\cdot\, i \sum_{i=1,2}^{\infty} \frac{2n_i+1}{n_i(n_i+1)}\,\frac{1}{r(r+1) - n_i(n_i+1)}\,\frac{1}{m(m+1) - n_i(n_i+1)}\,\frac{dn_i}{d\theta_o}\,\frac{S'_{n_i}(k\ell)}{S_{n_i}(k\ell)}\,.$$

(II-10)

where $\dfrac{\partial Ln_i}{\partial\theta_o}\Big/\dfrac{\partial Ln_i}{\partial n_i} = -\dfrac{dn_i}{d\theta_o}$

This equation is the r^{th} row of an infinite set of simultaneous equations. The b_r coefficients in the above expression should be multiplied by a constant, related to the amplitude of the source. For simplicity this constant was chosen to be one. This is permissible here since we are interested in the input impedance of the biconical antenna. However when the expressions for the electromagnetic field are examined, a dependence on the strength of the source should be present.

This set of simultaneous equations presents the second stumbling block in the theory of biconical antennas. It is seen that it would be advantageous to obtain n_i as a function of θ_o, then $\frac{dn_i}{d\theta_o}$ could be obtained by a differentiation. Robin and Pereira-Gomes [5] infinite series expressions for n_i become excessively lengthy when a continuous expression for $\frac{dn_i}{d\theta_o}$ is desired. A simpler expression for n_i would be much more applicable. Thus, the first step in this analysis of the biconical antenna was to find a simpler expression for n_i as a function of θ_o.

Since a solution of an infinite set of simultaneous equations is impossible, a truncated set is usually solved. The accuracy that one achieves with this method is limited only by the ability to invert large order matrices. The accuracy of the various truncated solutions can then be judged from the rate of convergence that the successive truncations show. Smith [3] limits himself to the first root n_1 and a second-order matrix, i.e. b_1 and b_3. The physical interpretation of this is that only the principal mode and the first are used to represent the field in the interior region. The application of a second-order matrix means that two modes are used to represent the exterior field and that only these modes have been used to match the two fields across the fictitious mathematical boundary. Robin and Pereira-Gomes [5] go one step further and use two roots n_1 and n_2 and then invert a 3 x 3 matrix, i.e. the matching is done with two interior and three exterior modes. Another difficulty is that tabulated values for the fractional order Bessel functions exists only for integer, half-integer, and third-integer orders. One can either find cone angles that will correspond to the indices for which the Bessel functions are tabulated, or one must calculate these Bessel functions from their basic definition.

Once the matrix is inverted or the values of b_m are known the load admittance can then be calculated from the expression [6, 3]

$$Y_L = \frac{120}{Z_o^2} \sum_{m=1,3}^{\infty} b_m \frac{1}{m(m+1)} P_m (\cos \theta_o) \qquad \text{(II-11)}$$

where Z_o is the characteristic impedance of an infinite biconical antenna (a structure like this is also a uniform transmission line for spherical waves) and is given by [6, 3]

$$Z_o = 120 \ln \cot \frac{\theta_o}{2} . \qquad \text{(II-12)}$$

In this approach the biconical antenna is considered as a piece of transmission line terminated by a load admittance Y_L which is the free space surrounding the antenna. The input impedance for the biconical antenna, which is the final goal in the analyses, can then be found from ordinary transmission line equations. The input impedance is then [6, 3]

$$Z_i = Z_o \frac{\cos k\ell + i Z_o Y_L \sin k\ell}{Y_L Z_o \cos k\ell + i \sin k\ell} \qquad \text{(II-13)}$$

III

THE ROOTS OF THE EQUATION $L_{n_i}(\theta_o) = 0$

We will now try to find a simple approximate solution for the eigenvalues n_i of the following Equation (II-4)

$$2L_{n_i}(\theta_o) = P_{n_i}(\cos\theta_o) - P_{n_i}(-\cos\theta_o) = 0 .$$

The accuracy of a solution can be juedged by comparing it to the results of Robin and Pereira-Gomes [5] which are accurate to three decimal places. These results of Robin and Pereira-Gomes [5] for the first eight roots of n_i will now be plotted.

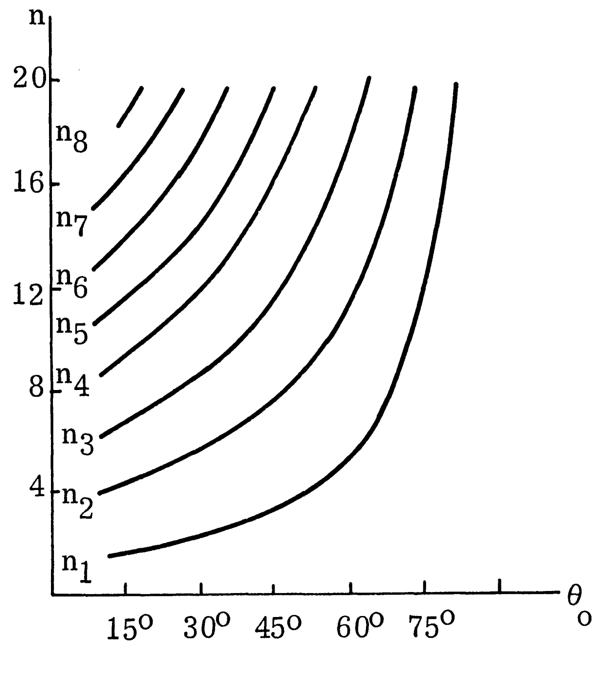

FIGURE 2. A GRAPH OF THE EIGENVALUES n_i OF EQUATION (II-4)

The first root n_1 for conical angles larger than 18^o is seen to be larger than two. This would suggest as a first attempt to obtain the roots n_i the use of asymptotic formulas for the Legendre functions of large order. In particular we have from Hobson [7], for $n \geq 1$ and θ_o confined to the interval $(\frac{1}{n}, \pi - \frac{1}{n})$

$$P_n(\cos\theta_o) = \left(\frac{2}{\pi \sin\theta_o}\right)^{1/2} \frac{\pi(n)}{\pi(n+\frac{1}{2})} \sin\left[(n+\frac{1}{2})\theta_o + \frac{\pi}{4}\right] + \mathcal{O}(\frac{1}{n^{3/2}}). \tag{III-1}$$

Substituting this asymptotic form in the characteristic equation for the roots n_i

$$P_{n_i}(\cos\theta_o) - P_{n_i}(-\cos\theta_o) = 0$$

we obtain to first order

$$\sin\left[(n+\frac{1}{2})\theta_o + \frac{\pi}{4}\right] - \sin\left[(n+\frac{1}{2})(\pi - \theta_o) + \frac{\pi}{4}\right] = 0.$$

Combining this trigonometrically, we get

$$\sin\left[(n+\frac{1}{2})(\frac{\pi}{2} - \theta_o)\right] = 0$$

which has for its solution

$$n_i = \frac{2\pi i}{\pi - 2\theta_o} - \frac{1}{2} \tag{III-2}$$

and

$$\frac{dn_i}{d\theta_o} = \frac{4\pi i}{(\pi - 2\theta_o)^2}. \tag{III-3}$$

This expression could be expected to give good results when n is large, but surprisingly it is very accurate for small values of n also. The following table can be used to compare the results obtained from this formula to the results obtained by Robin and Pereira-Gomes [5]. Each square in the table gives three values. The first value is taken from a similar table by Robin and Pereira-Gomes. The second value is computed from the above expression for n_i. The third value in each square is calculated from the above formula with a second-order correction term added and will be explained later in this section.

The value which shows the greatest error is as expected the first root, calculated for the smallest conical angel of $\theta_o = \frac{\pi}{12}$. Thus, the asymptotic expressions for large values of n which were used yield accuracy within one decimal place when n is as small as two. To obtain better accuracy we will include the second-order terms in the asymptotic expressions for the Legendre functions. The various asymptotic series in Hobson had to be carefully chosen, since all of them but one yielded larger errors for n_i when the next higher term in the series was included. The higher order correction terms of the various asymptotic series oscillate about the exact value for n_i. The simple first-order formula gives results which are so close to the exact value that unless many higher order terms are included the simple formula gives better results. However, one particular asymptotic expression for the Legendre function when

TABLE I. ROOTS OF THE EQUATION $P_{n_i}(\cos\theta_o) - P_{n_i}(-\cos\theta_o) = 0$

n_i \ θ_o	$\pi/12$	$\pi/6$	$\pi/4$	$\pi/3$	$5\pi/12$
n_1	1.793 1.900 1.795	2.43 2.50 2.448	3.462 3.500 3.468	5.477 5.500 5.480	11.489 11.500 11.490
n_2	4.244 4.300 4.239	5.467 5.500 5.470	7.480 7.500 7.482	11.489 11.500 11.489	23.495 23.500 23.495
n_3	6.657 6.700 6.657	8.478 8.500 8.479	11.487 11.500 11.488	17.492 17.500 17.493	35.496 35.500 35.496
n_4	9.066 9.100 9.066	11.483 11.500 11.484	15.490 15.500 15.491	23.494 23.500 23.494	47.497 47.500 47.497
n_5	11.472 11.500 11.473	14.486 14.500 14.487	19.492 19.500 19.492	29.495 29.500 29.495	59.498 59.500 59.498
n_6	13.876 13.900 13.877	17.489 17.500 17.489	23.493 23.500 23.494	35.496 35.500 35.496	71.498 71.500 71.498
n_7	16.279 16.300 16.280	20.490 20.500 20.491	27.494 27.500 27.494	41.497 41.500 41.497	83.498 83.500 83.498
n_8	18.682 18.700 18.682	23.491 23.500 23.492	31.495 31.500 31.495	47.497 47.500 47.497	95.499 95.500 95.499

The first value in each window is from a paper by Robin and Pereira-Gomes. The second value is calculated by the formula $n_i = 2\pi i/\pi - 2\theta_o - 1/2$. The third value is calculated from the above formula with a second-order correction term added.

used gave significant corrections to the simple formula. This expression from Hobson is:

$$P_n(\cos\theta) = \left(\frac{2}{\pi\sin\theta}\right)^{1/2} \frac{\pi(n)}{\pi(n+\frac{1}{2})} \left\{\cos\left[(n+\frac{1}{2})\theta - \frac{\pi}{4}\right] + \frac{1}{2(2n+3)} \frac{\cos\left[(n+\frac{3}{2})\theta - \frac{3\pi}{4}\right]}{2\sin\theta}\right\}$$

$$+ \mathcal{O}\left(\frac{1}{n^{5/2}}\right) \ldots \frac{1}{n} \leqslant \theta \leqslant \pi - \frac{1}{n} \qquad \text{(III-4)}$$

Thus

$$P_{n_i}(\cos\theta_o) - P_{n_i}(-\cos\theta_o) = 0$$

becomes

$$\cos\left[(n+\frac{1}{2})\theta_o - \frac{\pi}{4}\right] + \frac{\cos\left[(n+\frac{3}{2})\theta_o - \frac{3\pi}{4}\right]}{4(2n+3)\sin\theta_o} - \cos\left[(n+\frac{1}{2})(\pi-\theta_o) - \frac{\pi}{4}\right] -$$

$$- \frac{\cos\left[(n+\frac{3}{2})(\pi-\theta_o) - \frac{3\pi}{4}\right]}{4(2n+3)\sin\theta_o} = 0, \quad \frac{1}{n} \leqslant \theta \leqslant \pi - \frac{1}{n} .$$

Combining this with the aid of trigonometric identities and simplifying we get

$$\sin(n+\frac{1}{2})(\frac{\pi}{2} - \theta_o) + \frac{1}{4(2n+3)\sin\theta_o} \sin(n+\frac{3}{2})(\frac{\pi}{2} - \theta_o) = 0 . \qquad \text{(III-5)}$$

To simplify further, the argument of the second sine term can be written as

$$n + \frac{3}{2} = n + \frac{1}{2} + 1 .$$

Combining again

$$\sin(n+\frac{1}{2})(\frac{\pi}{2}-\theta_o) + \frac{1}{4(2n+3)} \left[\cot\theta_o \cos(n+\frac{1}{2})(\frac{\pi}{2}-\theta_o) + \sin(n+\frac{1}{2})(\frac{\pi}{2}-\theta_o)\right] = 0\,. \tag{III-6}$$

The first part of this result when equated to zero is the simple formula (III-2) arrived at before. We will write its solution as n_i^o. The second part which includes all the $1/n$ terms will be the correction to the simple formula. Therefore let us write

$$n_i = n_i^o - \delta_i \tag{III-7}$$

where δ_i is small. When this is substituted in the above formula we get

$$\sin(\frac{\pi}{2}-\theta_o)\delta_i + \frac{1}{8(n_i^o-\delta_i)+12} \left[\sin(\frac{\pi}{2}-\theta_o)\,\delta_i - \cot\theta_o \cos(\frac{\pi}{2}-\theta_o)\,\delta_i\right] = 0. \tag{III-8}$$

Since δ_i is small we can make the following approximations in the above expression

$$n_i^o - \delta_i \approx n_i^o$$

$$\sin(\frac{\pi}{2}-\theta_o)\,\delta_i \approx (\frac{\pi}{2}-\theta_o)\,\delta_i$$

$$\cos(\frac{\pi}{2}-\theta_o)\,\delta_i \approx 1.$$

The sine term inside the square bracket can also be neglected with respect to the cosine term. Then we get

$$\delta_i = \frac{2}{\pi - 2\theta_o} \frac{\cot\theta_o}{8n_i^o + 12} . \tag{III-9}$$

Substituting for n_i^o we get

$$\delta_i = \frac{\cot\theta_o}{8\pi i + 4(\pi - 2\theta_o)} . \tag{III-10}$$

The roots, correct to second order, are now

$$n_i = \frac{2\pi i}{\pi - 2\theta_p} - \frac{1}{2} - \frac{\cot\theta_o}{8\pi i + 4(\pi - 2\theta_o)} \tag{III-11}$$

and

$$\frac{dn_i}{d\theta_o} = \frac{4\pi i}{(\pi - 2\theta_o)^2} + \frac{8\cot\theta_o + \left[8\pi i + 4(\pi - 2\theta_o)\right]\csc^2\theta_o}{\left[8\pi i + 4(\pi - 2\theta_o)\right]^2} . \tag{III-12}$$

The third value for n_i in each square of the Table I was computed using this expression. The largest error of these values when compared to those of Robin and Pereira-Gomes is approximately one-half of a percent.

IV

ORDER RESTRICTION OF THE EXTERIOR MODE COEFFICIENTS b_m

In this section we will try to find the behavior of the sequence of b_m coefficients, assuming only that the series representation for the average complex power flow W must be convergent. Thus, for a physically realizable source, the average complex power flow W must be

$$W < \infty .$$

In a spherical coordinate system the average complex power flow is given by

$$W = \iint \hat{r} \cdot \bar{S} \, dA \tag{IV-1}$$

where $\bar{S}$ is the Poynting's vector

$$\bar{S} = \frac{1}{2} \operatorname{Re} (\bar{E} \times \bar{H}^{*}) \tag{IV-2}$$

and $\hat{r}$ is the unit radial vector. More explicitly

$$W = \frac{1}{2} \int_0^{2\pi} \int_0^{\pi} E_\theta \, H_\phi^{*} \, r^2 \sin\theta \, d\theta \, d\phi . \tag{IV-3}$$

The electric field E_θ is given by equation (II-1)

$$E_\theta = \frac{\eta}{i\, 2\pi r} \sum_m \frac{b_m}{m(m+1)} \frac{R'_m(kr)}{R_m(k\ell)} \frac{d}{d\theta} P_m(\cos\theta)$$

and the magnetic field H_ϕ [6] is

$$H_{\phi}^{\#} = \frac{-1}{2\pi r} \sum_m \frac{b_m^{\#}}{m(m+1)} \frac{R_m^{\#}(kr)}{R_m^{\#}(k\ell)} \frac{d}{d\theta} P_m(\cos\theta) \qquad \text{(IV-4)}$$

When these are substituted in equation (IV-3) the average complex power flow becomes

$$W = \frac{i\eta}{4\pi} \int_0^{\pi} \left(\sum_m \frac{b_m}{m(m+1)} \frac{R'_m}{R_m} P'_m \right) \left(\sum_r \frac{b_r^{\#}}{r(r+1)} \frac{R_r^{\#}}{R_r^{\#}} P'_r \right) \sin\theta \, d\theta \, . \qquad \text{(IV-5)}$$

Using the orthogonal properties of the Legendre functions which are

$$\int_0^{\pi} \frac{dP_m(\cos\theta)}{d\theta} \frac{dP_r(\cos\theta)}{d\theta} \sin\theta \, d\theta = \begin{cases} 0 \, , & m \neq r \\ \dfrac{2m(m+1)}{2m+1} \, , & m = r \end{cases} \, . \qquad \text{(IV-6)}$$

Equation (IV-5) reduces to

$$W = \frac{i\eta}{2\pi} \sum_m \left| b_m \right|^2 \frac{1}{m(m+1)(2m+1)} \frac{R'_m(kr) \, R_m^{\#}(kr)}{\left| R_m(k\ell) \right|^2} \, . \qquad \text{(IV-7)}$$

In the limit as $m \to \infty$,

$$\frac{R'_m(kr) \, R_m^{\#}(kr)}{\left| R_m(k\ell) \right|^2} \sim m \, . \qquad \text{(IV-8)}$$

Thus, the expression for the average complex power flow in the limit as $m \to \infty$ behaves like the series

$$\sum_m \left| b_m \right|^2 \frac{1}{m^2} \, . \qquad \text{(IV-9)}$$

For this series to be converging, $|b_m|^2$ cannot go faster to infinity than

$$|b_m|^2 \sim m^{1-\epsilon} \qquad \epsilon > 0 . \tag{IV-10}$$

The mode coefficients b_m must therefore have the property

$$|b_m| \leqslant m^{\frac{1}{2}-\frac{\epsilon}{2}} . \tag{IV-11}$$

V

ORDER BEHAVIOUR OF OTHER EXPRESSIONS

We shall examine now the order behaviour of some other expressions which involve b_m either directly or indirectly.

The matrix expression for b_m, equation (II-10), can be rewritten as

$$b_r = -iP_r(2r+1)\frac{R_r}{R'_r}\left[1+ir(r+1)\sum_m b_m P_m \sum_i \frac{2n_i+1}{n_i(n_i+1)}\,\frac{1}{r(r+1)-n_i(n_i+1)}\cdot\right.$$

$$\left.\cdot\frac{1}{m(m+1)-n_i(n_i+1)}\,\sin\theta_o\,\frac{dn_i}{d\theta_o}\,\frac{S'_{n_i}}{S_{n_i}}\right]. \qquad \text{(V-1)}$$

The behaviour of this when $r \rightarrow \infty$ is

$$b_r \sim -iP_r\,(2r+1)\,\frac{R_r}{R'_r} \qquad \theta_o > 0\,. \qquad \text{(V-2)}$$

Since

$$\lim_{r\rightarrow\infty} P_r \sim \frac{1}{\sqrt{r}}$$

and

$$\lim_{r\rightarrow\infty} \frac{R_r}{R'_r} \sim \frac{1}{r}\,.$$

Then b_r, as $r \rightarrow \infty$, behaves like

$$b_r \sim \frac{1}{\sqrt{r}} \tag{V-3}$$

This is well within the restrictions of equation (IV-11).

The i-sum in the expression of b_r (V-1) is

$$\sum_i \frac{2n_i+1}{n_i(n_i+1)} \; \frac{1}{r(r+1)-n_i(n_i+1)} \; \frac{1}{m(m+1)-n_i(n_i+1)} \sin\theta_o \frac{dn_i}{d\theta_o} \frac{S'_{n_i}}{S_{n_i}} \; .$$

As $n_i \to \infty$, this sum behaves like the sum

$$\sum_i \frac{1}{n_i^3} \; . \tag{V-4}$$

since from equation (III-3)

$$\lim_{n_i \to \infty} \sin\theta_o \frac{dn_i}{d\theta_o} \sim n_i \tag{V-5}$$

and

$$\lim_{n_i \to \infty} \frac{S'_{n_i}}{S_{n_i}} \sim n_i \; . \tag{V-6}$$

The rapid convergence of the i-sum in equation (V-4) should be noted. This guarantees that for large cone angles θ_o, when n_i is large, the i-sum is reasonably approximated by the first few terms of the i-sum.

The next expression to be examined is that for the load admittance Y_L given by equation (II-11)

$$Y_L = \frac{120}{Z_o^2} \sum_{m=1,3}^{\infty} b_m \frac{1}{m(m+1)} P_m (\cos \theta_o) . \tag{II-11}$$

As $m \rightarrow \infty$, the terms in the sum for the load admittance Y_L behave as

$$b_m P_m \frac{1}{m(m+1)} \sim \frac{1}{m^3} . \tag{V-7}$$

This was derived using equation (V-3) and the asymptotic expression for the Legendre functions.

The very important conclusion that can be drawn from the behaviour of the above expression is that the load admittance Y_L will be determined by the first few exterior modes. Generally, considering the rapid convergence of equation (II-11), the load admittance can be determined as accurately as desired by the first few N-terms of the series

$$Y_L \approx \frac{120}{Z_o^2} \sum_{m=1,3}^{N} b_m \frac{1}{m(m+1)} P_m (\cos \theta_o) . \tag{V-8}$$

Thus, in any scheme to obtain the exterior mode coefficients b_m, one should pay particular attention to the accuracy of the first mode. Larger errors can be tolerated in the higher modes without affecting greatly the overall accuracy of the load admittance.

VI

SOLUTION OF THE SIMULTANEOUS EQUATIONS BY TRUNCATING THE INFINITE SET

If the characteristic values n_i are known the next step in the solution of the biconical antenna would be to solve for the coefficients b_m. The usual method of attack is to truncate the infinte set and solve the finite equations for b_m. Even this is difficult since the terms of the matrix are complex and each term contains another infinite sum which again will have to be truncated. Re-writing the matrix for b_m, equation (II-10), in a condensed notation as

$$A_r + \alpha_r b_r = \sum_m b_m P_m N_r^m \tag{VI-1}$$

where

$$N_r^m = \sin\theta_o \sum_{i=1}^{\infty} \frac{2n_i+1}{n_i(n_i+1)} \frac{1}{n_i(n_i+1)-r(r+1)} \frac{1}{n_i(n_i+1)-m(m+1)} \frac{dn_i}{d\theta_o} \frac{S'_{n_i}(k\ell)}{S_{n_i}(k\ell)}, \tag{VI-2}$$

it is readily seen that before one can solve for the unknown coefficients b_m, the series given by N_r^m will have to be summed first. The most accurate solution to date was carried out by Robin and Pereira-Gomes [5] who approximated N_r^m for each r and m by its first two terms (i.e. i = 1, 2) and then solved for b_1, b_3, and b_5 by inverting a three by three matrix.

If one were to use this truncation method in the solution for the mode coefficients b_m it would be desirable to invert a matrix of the highest order and to include as many terms as possible in calculating N_r^m. A summation technique will now be applied to N_r^m which will give its sum accurately by the first few terms of a transformed series.

A. A Summation Technique Applied to N_r^m

We will now apply Kummer's summation technique [8] to N_r^m. The roots n_i will be given by the simple formula, equation (III-2), and $\frac{dn_i}{d\theta_o}$ by equation (III-3). If more accurate results are desired the more exact solution for the first few roots of n_i can be included. To simplify notation, let equation (III-2) be written as

$$n_i = \rho\, i - \frac{1}{2} \qquad \text{(VI-3)}$$

where

$$\rho = \frac{2\pi}{\pi = 2\theta_o} \, .$$

After making this substitution and combining algebraically, the above summation becomes

$$\frac{N_r^m}{\sin\theta_o} = \frac{2}{\pi\rho^3} \sum_{i=1}^{\infty} \frac{i^2}{\left(i^2 - \frac{1}{4\rho^2}\right)\left(i^2 - \frac{1}{\rho^2}\left[\frac{1}{4} + r(r+1)\right]\right)\left(i^2 - \frac{1}{\rho^2}\left[\frac{1}{4} + m(m+1)\right]\right)} \frac{S'_{n_i}(k\ell)}{S_{n_i}(k\ell)} \, . \qquad \text{(VI-4)}$$

Now let

$$a^2 = \frac{1}{4\rho^2}$$

$$b^2 = \frac{1}{\rho^2}\left[\frac{1}{4} + r(r+1)\right]$$

$$c^2 = \frac{1}{\rho^2}\left[\frac{1}{4} + m(m+1)\right] .$$

The ratio S'/S can be rewritten as

$$\frac{S'_{n_i}(k\ell)}{S_{n_i}(k\ell)} = \frac{n_i}{k\ell} - \frac{J_{n_i+1}{}^{\prime}(k\ell)}{J_{n_i}(k\ell)} = \frac{\rho i}{k\ell} - \frac{1}{2k\ell} - \frac{J_{n_i+1}(k\ell)}{J_{n_i}(k\ell)} . \tag{VI-5}$$

The above sum can now be re-expressed as three sums, i.e.

$$\frac{2}{\pi\rho^2 k\ell}\sum_{i=1}^{\infty}\frac{i^3}{(i^2-a^2)(i^2-b^2)(i^2-c^2)} - \frac{1}{\pi\rho^3 k\ell}\sum_{i=1}^{\infty}\frac{i^2}{(i^2-a^2)(i^2-b^2)(i^2-c^2)}$$

$$-\frac{2}{\pi\rho^3}\sum_{i=1}^{\infty}\frac{i^2}{(i^2-a^2)(i^2-b^2)(i^2-c^2)}\;\frac{J_{n_i+1}(k\ell)}{J_{n_i+1}(k\ell)} . \tag{VI-6}$$

The first two sums can be summed in closed form with the aid of the series

$$\sum_{i=1}^{\infty}\left(\frac{1}{i} - \frac{1}{x+i}\right) = \psi(x) + \frac{1}{x} + \gamma \tag{VI-7}$$

where γ is Euler's constant and $\psi(x)$ is the logarithmic derivative of the gamma function $\Gamma(x)$. Therefore, the first sum in closed form is

$$\frac{1}{\pi \rho^2 k\ell} \left\{ \frac{a^2}{(a^2-b^2)(c^2-a^2)} \left[\psi(a)+\psi(-a)\right] + \frac{b^2}{(a^2-b^2)(b^2-c^2)} \left[\psi(b)+\psi(-b)\right] \right.$$

$$\left. + \frac{c^2}{(c^2-a^2)(b^2-c^2)} \left[\psi(c)+\psi(-c)\right] \right\} \qquad \text{(VI-8)}$$

and the second sum in closed form is

$$\frac{-1}{2\pi \rho^3 k\ell} \left\{ \frac{a}{(a^2-b^2)(a^2-c^2)} \left[\psi(a)-\psi(-a)\right] + \frac{b}{(a^2-b^2)(c^2-b^2)} \left[\psi(b)-\psi(-b)\right] \right.$$

$$\left. + \frac{c}{(c^2-a^2)(c^2-b^2)} \left[\psi(c)-\psi(-c)\right] \right\}. \qquad \text{(VI-9)}$$

The third sum cannot be expressed in closed form; the best that can be done is to use a summation technique. We will apply Kummer's [8] transformation to make the series more rapidly convergent. Thus, since the term $\frac{J_{n_i+1}(k\ell)}{J_{n_i}(k\ell)}$ is of order $1/i$ as n_i gets large, i.e.

$$\lim_{i \to \infty} \frac{J_{n_i+1}(k\ell)}{J_{n_i}(k\ell)} = \frac{k\ell}{2} \frac{1}{n_i+1} \qquad \text{(VI-10)}$$

we will want to sum in closed form the special series

$$\sum_{i=1}^{\infty} \frac{i}{(i^2-a^2)(i^2-b^2)(i^2-c^2)} = \Omega$$

Using the same techniques as for the first two sums, the special series can be given as

$$\frac{1}{2}\,\frac{1}{(a^2-b^2)(c^2-a^2)}\Big[\psi(a)+\psi(-a)\Big]+\frac{1}{2}\,\frac{1}{(a^2-b^2)(b^2-c^2)}\Big[\psi(b)+\psi(-b)\Big]$$

$$+\frac{1}{2}\,\frac{1}{(a^2-c^2)(c^2-b^2)}\Big[\psi(c)+\psi(-c)\Big]=\Omega\,.$$

The convergence factor of Kummer's [8] technique for the third sum is

$$\xi=\lim_{i\to\infty}\, i\,\frac{J_{n_i+1}(k\ell)}{J_{n_i}(k\ell)}=\frac{k\ell}{2\rho}\;.$$

Therefore the third sum can now be expressed [8] as

$$-\frac{2}{\pi\rho^3}\left\{\frac{k\ell}{2\rho}\,\Omega+\sum_{i=1}^{\infty}\left(1-\frac{k\ell}{2\rho}\,\frac{1}{i}\,\frac{J_{n_i}(k\ell)}{J_{n_i+1}(k\ell)}\right)\frac{i^2}{(i^2-a^2)(i^2-b^2)(i^2-c^2)}\,\frac{J_{n_i+1}(k\ell)}{J_{n_i}(k\ell)}\right\}. \qquad \text{(VI-11)}$$

The real advantage of this summation technique is that it converts the series N_r^m which behaves asymptotically like the series

$$\sum_i \mathcal{O}\left(\frac{1}{n_i^3}\right)$$

to a more rapidly converging series of order

$$\sum_i \mathcal{O}\left(\frac{1}{n_i^6}\right) .$$

To summarize, let us retrace the steps which should clarify the procedure. The infinite set of simultaneous equations (II-10) was rewritten in an abbreviated form

$$A_r + \alpha_r b_r = \sum_m P_m N_r^m b_m \tag{VI-1}$$

where r denotes the row of the matrix and m the column (r, m = 1, 3, 5...) and N_r^m is given by equation (VI-2). N_r^m was then broken up into three simpler sums, the first two of which could be expressed in closed form. Kummer's summation technique was applied to the third sum. Each summation index i can be identified with one interior mode (as each summation index m can be identified with one exterior mode). However, after applying a summation technique to N_r^m no clear statement can be made on the number of interior modes that have been included. The summation technique procedure for N_r^m "mixes up" the interior modes in order to increase the convergence.

Having calculated N_r^m for each r and m, the matrix can then be inverted. To determine the accuracy of the inversion a truncation of the next higher order can be made, this matrix then inverted and the results compared to the previous truncation. If the results of these two truncations are very different, higher order truncations must be made. With the b_m coefficients known, one can express the input impedance and radiated field for the biconical antenna.

Since the matching of the fields of two different regions with different orthogonal ranges introduces a matrix for one of the coefficients of the two fields, there is no way to escape a matrix inversion. The matrix indicates that in an exact solution all modes of one field have an effect upon all modes of the other field. Ideally then, one should match all interior modes to all exterior modes. In the matching process, arbitrarily many interior modes can be used, since a summation technique over n_i is applied. However, to include all exterior modes it would be necessary to invert an infinite matrix. Thus the ultimate goal to match all interior to all exterior modes is limited only by the ability to invert a high-order matrix. As the cone angle $\theta_o \longrightarrow 0^o$, the modes decouple, i.e. $a_n = b_m$, and all that is left is to crossmatch modes of like order in the two regions. Cross-coupling between different modes comes in only as a perturbation which dies out as $\theta_o \longrightarrow 0^o$. Mathematically the matrix for b_m decouples so that each b_m is a known function, and instead of the matrix equation for b_m we now have equation (IX-8).

Returning to the wide angle cone we know from physical intuition that the amplitudes of the higher modes must diminish as the order increases for a finite energy input to the system. This guarantees that the m + 1 exterior mode for m large, will contribute only a small correction term in the exterior field expression. Since the cross-coupling between interior and exterior modes is maximum for modes of the same order, and since the interaction between different modes diminishes as the index difference increases, there is no real point to include all the interior modes when only a small number of exterior modes (given by the order of the matrix) are used. In other words, the results that are obtained by including all interior modes and only a few exterior modes are as valid as the results obtained by taking into account a few interior modes and a few exterior modes. However, in the analysis no particular difficulty would be experienced in using many interior modes, since a summation technique can be applied to the interior modes.

B. A Comment on the Accuracy of a Three-by-Three Truncation

As pointed out before the highest order truncation to date was made by Robin and Pereira-Gomes [5]. They truncated the infinite set to a 3 x 3 matrix and then inverted it. The coefficients in the matrix which are given by infinite series were approximated by the first two terms of the series. To see how good this truncation is it was decided to invert a 5 x 5 matrix and compare the results thus obtained to the results of the 3 x 3 truncation. For these calculations the cones were chosen to have an angle $\theta_0 = 30^{\circ}$, and length ka = 1. The coefficients in the matrix were now approximated by the first four terms of the series. This gave five-decimal accuracy for the coefficients.

The 3 x 3 matrix is given by equation (VI-1) as

$$\begin{aligned}
iP_1 &= \left(2P_1^2 N_1^1 - \frac{1}{3}\frac{R'_1}{R_1}\right) b_1 + (2P_1 P_3 N_1^3) b_3 + (2P_1 P_5 N_1^5) b_5 \\
iP_3 &= \left(12P_3 P_1 N_3^1\right) b_1 + \left(12P_3^2 N_3^3 - \frac{1}{7}\frac{R'_3}{R_3}\right) b_3 + (12P_3 P_5 N_3^5) b_5 \qquad \text{(VI-12)} \\
iP_5 &= (30P_5 P_1 N_5^1) b_1 + (30P_5 P_3 N_5^3) b_3 + \left(30P_5^2 N_5^5 - \frac{1}{11}\frac{R'_5}{R_5}\right) b_5
\end{aligned}$$

To reproduce Robin's results the coefficients for the above 3 x 3 matrix were approximated by the first two terms in the series. Thus with the numerical values substituted the above set of simultaneous equations becomes

$$\begin{aligned}
i.8660 &= (.3054 + i.1667)b_1 + (-0797)b_3 + (-.0038)b_5 \\
i.3248 &= (-.4780)b_1 + (.7390 + i.0005)b_3 + (-.0817)b_5 \qquad \text{(VI-13)} \\
-i.2233 &= (-.0569)b_1 + (-.2045)b_3 + (.7825)b_5
\end{aligned}$$

The solutions of this set are

$$b_1 = 1.650 + i2.490, \; b_3 = 1.108 + i2.096, \; b_5 = .409 + i.444. \qquad \text{(VI-14)}$$

Approximating the coefficients by the first four terms in the series, the 5 x 5 matrix is

$$\begin{bmatrix} i.8660 \\ i.3248 \\ -i.2233 \\ -i.4102 \\ -i.1896 \end{bmatrix} = \begin{bmatrix} (.3088 + i.16666) & (-.0783) & (-.00508) & (.01028) & (.00656) \\ (-.470) & (.7477 + i.000516) & (-.0841) & (-.02222) & (.00358) \\ (-.0764) & (-.2105) & (.791) & (-.1208) & (-.0448) \\ (.2875) & (-.1038) & (-.226) & (.794) & (-.1308) \\ (.2955) & (.0255) & (-.1342) & (-.1995) & (.991) \end{bmatrix} \begin{bmatrix} b_1 \\ b_3 \\ b_5 \\ b_7 \\ b_9 \end{bmatrix} . \tag{VI-15}$$

The solutions of this are

$$\begin{aligned} b_1 &= 1.648 + i\,2.493 \\ b_3 &= 1.065 + i\,1.993 \\ b_5 &= .341 + i\,.222 \\ b_7 &= -.453 + i\,1.296 \\ b_9 &= -.564 - i\,1.217 \end{aligned} \tag{VI-16}$$

Thus, there is close agreement between the b's as obtained from the 3 x 3 and the 5 x 5 matrix for the first two values of b. This points out the validity of the truncation method to obtain the coefficients b_r when only the impedance for a biconical antenna is desired. In Section V, equation (V-8), it was concluded that the first few values of the exterior mode coefficients b are the most important ones. However, as higher order truncations are made the accuracy of the first few values of b also improves, thus increasing the accuracy of the impedance expression.

A somewhat different answer will be obtained from the 3 x 3 matrix when the coefficients are given by the first four terms in the series instead of only two. This 3 x 3 matrix is then

$$\begin{aligned} i.8660 &= (.3088 + i.1667)b_1 - .0783\, b_3 - .00508\, b_5 \\ i.3248 &= -.470\, b_1 + (.7477 + i.000516)b_3 - .0841\, b_5 \\ -i.2233 &= -.0764\, b_1 - .2105\, b_3 + .791\, b_5\,. \end{aligned} \tag{VI-17}$$

The solutions to this set are

$$\begin{aligned} b_1 &= 1.507 + i\,2.335 \\ b_3 &= .972 + i\,1.88 \\ b_5 &= .404 + i\,.444\,. \end{aligned}$$

There is a small difference between these answers and the ones obtained from the matrix equations (VI-13). However, it is difficult to say which of the two answers is more correct since the largest error is introduced by the truncation to a 3 x 3 matrix.

C. A Method of Truncation

It was shown in Section V that we are really interested in only the first few mode coefficients b_r. One arrives at this conclusion after examining the expression for the load admittance

$$Y_L = \frac{120}{Z_o^2} \sum_{m=1}^{N} \frac{P_m \, b_m}{m(m+1)} . \qquad \text{see (II-11)}$$

In a numerical evaluation Y_L can be found as accurately as desired by a finite sum

$$Y_L \approx \frac{120}{Z_o^2} \sum_{m=1}^{N} \frac{P_m \, b_m}{m(m+1)} \qquad \text{see (V-8)}$$

The rapid convergence of the first series above for Y_L guarantees this approximation. Hence, let us see if we can extract a finite matrix [9] from the infinite set that would give the first N-values for b. Using a compact notation for equation (II-10), which is more suitable here than the condensed notation adapted in equation (VI-1) for truncating matrices one can write the set of infinite simultaneous equations that determine b_r as

$$B_r = b_r - \sum_{m=1}^{\infty} I_r^m b_m . \qquad \text{(VI-18)}$$

Separating the remainder of the sum we get

$$B_r + \sum_{m=N+2}^{\infty} I_r^m b_m = b_r - \sum_{m=1}^{N} I_r^m b_m . \tag{VI-19}$$

If the exact values for b_m when m is large were known we could calculate the remainder of the series and thus obtain a corrected free member B'_r (source term), where B'_r is now

$$B'_r = B_r + \sum_{N+2}^{\infty} I_r^m b_m \tag{VI-20}$$

such that the truncated set

$$B'_r = b_r - \sum_{m+1}^{N} I_r^m b_m \tag{VI-21}$$

will give the exact values for $b_1, b_3, \ldots b_N$.

Equation (VII-6) is a series expression for b_r obtained by successive approximations. Taking the limit as b_r approaches infinity of this expression we obtain

$$\lim_{r \to \infty} b_r = B_r \qquad \theta_o > 0 . \tag{VI-22}$$

Assuming that this is a good approximation for b_r when r is large, we can use this now in evaluating B'_r. Thus, the corrected free member B'_r is

$$B'_r = B_r + \sum_{N+2}^{\infty} I_r^m B_m . \tag{VI-23}$$

Equation (VI-21) can now be solved to obtain the first N-values of b as accurately as desired by letting N become very large. In the limit as N approaches infinity,

$$\lim_{N \to \infty} B'_r = B_r \qquad \text{(VI-24)}$$

and thus equation (VI-21) becomes equation (VI-18).

VII

SOLUTIONS BY THE METHOD OF SUCCESSIVE APPROXIMATIONS

The method of successive approximations can be applied to obtain solutions to the infinite set of simultaneous equations for b_r. Equation (VI-1) stated again is

$$b_r = -\frac{A_r}{\alpha_r} + \frac{1}{\alpha_r} \sum_{m=1}^{\infty} P_m N_r^m b_m \tag{VI-1}$$

Writing this in a more useful form for successive approximations

$$b_r = B_r + \sum_m I_r^m b_m \tag{VII-1}$$

where

$$B_r = -\frac{A_r}{\alpha_r} = -i P_r (2r+1) \frac{R_r}{R'_r} \tag{VII-2}$$

$$\alpha_r = \frac{1}{P_r r(r+1)(2r+1)} \frac{R'_r}{R_r} \tag{VII-3}$$

$$I_r^m = \frac{1}{\alpha_r} P_m N_r^m . \tag{VII-4}$$

N_r^m is given by equation (VI-2).

There are many ways by which a series representation for b_r based on the method of successive approximations can be developed. Perhaps the most apparent one is that obtained by repeatedly substituting the exact equation (VII-1) for b_r into itself, thus

$$b_r = B_r + \sum_m I_r^m \left(B_m + \sum_k I_m^k \left(B_k + \sum_\ell I_k^\ell \left(B_\ell \cdots\right.\right.\right. \tag{VII-5}$$

$$= B_r + \left(\sum_m I_r^m\right) B_m + \left(\sum_m I_r^m\right)\left(\sum_k I_m^k\right) B_k + \left(\sum_m I_r^m\right)\left(\sum_k I_m^k\right)\left(\sum_\ell I_k^\ell\right) B_\ell + \cdots$$

If this is continued indefinitely and the series converges (if it converges it must converge to b_r) we have now b_r explicitly, i.e.

$$b_r = \sum_{\gamma=0}^{\infty} b_r^{(\gamma)} \tag{VII-6}$$

where

$$b^{(0)} = B_r$$

and

$$b_r^{(\gamma)} = \sum_m I_r^m \, b_r^{(\gamma-1)} \quad . \tag{VII-7}$$

The same series for b_r can be developed using a different approach. Equation (VII-1) is the r^{th} row of an infinite matrix which characterizes b_r. Writing this in operational form we get for b_r

$$b = B + Ib \tag{VII-8}$$

or

$$\left[1 - I\right] b = B.$$

This matrix can now be solved for b by multiplying both sides by the inverse of the matrix, thus

$$b = \left[1 - I\right]^{-1} B \quad . \qquad \text{(VII-9)}$$

If the norm of I satisfies

$$\| I \| < 1 \qquad \text{(VII-10)}$$

we can expand the inverse of the matrix and write b as follows

$$b = \left[1 + I + I^2 + I^3 + \ldots\right] B \qquad \text{(VII-11)}$$

but this is identical to equation (VII-5).

As will be shown in a later section (IX) for very thick cones

$$\lim_{\theta_o \to \frac{\pi}{2}} b_r = B_r = - i P_r (2r + 1) \frac{R_r}{R'_r} \qquad \text{(VII-12)}$$

since

$$\lim_{\theta_o \to \frac{\pi}{2}} I_r^m = 0 \qquad \text{(VII-13)}$$

and for infinitesimally thin cones

$$\lim_{\theta_o \to 0} b_r = \frac{\pi}{2} (2r+1) S_r R_r \tag{VII-14}$$

since

$$\lim_{\theta_o \to 0} I_r^m = \begin{cases} 0 & , \; r \neq m \neq i \\ \dfrac{R_r}{R'_r} \dfrac{S'_r}{S_r} & , \; r = m = i \end{cases} \; . \tag{VII-15}$$

Thus, for thick cones a good approximation to the solution b_r, can be obtained by the first few terms of the series as given by equation (VII-6), but for thin cones more and more terms must be included to get reasonable accuracy for b_r. It can be shown in the limit as $\theta_o \to 0$ that all terms of the series solution given by equation (VII-6) must be included. This becomes apparent when the limit, as $\theta_o \to 0$ of I_r^m, equation (VII-15), is substituted in the solution for b_r (equation VII-6); hence

$$\lim_{\theta_o \to 0} b_r = B_r \sum_{\gamma=0}^{\infty} \left(\frac{R_r}{R'_r} \frac{S'_r}{S_r} \right)^{\gamma}$$

$$= B_r \frac{1}{1 - \dfrac{R_r S'_r}{R'_r S_r}} \tag{VII-16}$$

$$= \frac{\pi}{2} (2r+1) S_r R_r \; . \qquad \text{identical to (VII-14)}$$

In the last step the value of the Wronskian was used which is

$$S_r R'_r - R_r S'_r = - \frac{2}{\pi} i . \qquad \text{(VII-17)}$$

Thus this particular method of successive approximations develops a very slowly converging series for thin cones.

An approximation by a series for b_r, which gives b_r accurately by its first few terms when θ_o approaches either 0 or $\pi/2$, was pointed out by Schelkunoff [10]. The key to this method is to rewrite the equation for b_r in such a way that when successive approximations are applied the first term in the series will be the exact solution to b_r for the two limiting cone angles. This can be deduced from equation (VII-15). It is noticed in this equation that for very thin cones the only terms that contribute are the terms for which r = m = i. Thus let us rewrite equation (VII-1) by taking out the r^{th} term under the summation sign and combining it with b_r on the left side of the equation, i. e.

$$b_r = \frac{1}{1 - I_r^r} \left(B_r + \sum_{m'} I_r^m \, b_m \right) \qquad \text{(VII-18)}$$

where the prime on the summation index m denotes the omission of the r^{th} term. For thick cones the convergence of this equation is not destroyed since

$$\lim_{\theta_o \to \frac{\pi}{2}} I_r^r = 0 .$$

Applying the method of successive approximations [9] to solve equation (VII-18) we get

$$b_r = \lim_{\gamma \to \infty} b_r^{(\gamma)} \qquad \text{(VII-19)}$$

where

$$b_r^{(\gamma)} = \frac{1}{1 - I_r^r} \left(B_r + \sum_{m'} I_r^m \, b_m^{(\gamma - 1)} \right) \qquad \text{(VII-20)}$$

and

$$b_r^{(0)} = \frac{B_r}{1 - I_r^r} . \qquad \text{(VII-21)}$$

The first approximation of $b_r^{(0)}$ is now the exact solution for thin cones ($\theta_o \longrightarrow 0$) and thick cones ($\theta_o \longrightarrow \frac{\pi}{2}$), since

$$\lim_{\theta_o \to 0} b_r^{(0)} = \lim_{\theta_o \to 0} \frac{B_r}{1 - I_r^r} = \frac{\pi}{2} (2r + 1) S_r R_r$$

which agrees with equation (VII-14), and

$$\lim_{\theta_o \to \frac{\pi}{2}} b_r = \lim_{\theta_o \to \frac{\pi}{2}} \frac{B_r}{1 - I_r^r}$$

$$= B_r$$

which agrees with equation (VII-12).

VIII

A DISCUSSION OF THE INTERIOR AND EXTERIOR MODES AND MODE MATCHING

Schelkunoff [1] in his paper shows the electric lines of force for various modes in free space and on conical transmission lines. His drawings indicate the change which occur in the electric lines of the free-space modes when conical conductors are introduced. Of course, in a biconical antenna where the cones are finite, both of these wave types occur. The free-space modes are "outside" the biconical antenna, and the conical transmission modes are in the interior region (region I in Fig. 1). The TEM mode, or the dominant mode exists only in the interior region where the electric lines can terminate on the conductors.

Pictures can also be drawn which display the mechanism of mode matching in the two regions. Most important, however, they show qualitatively the changes in coupling between the modes of the two regions as the cone angle varies.

For thin cones the mode picture can be drawn as follows:

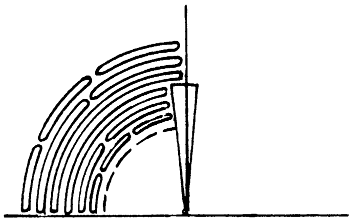

FIGURE 3. EXTERIOR AND INTERIOR MODES FOR THIN CONES*

For simplicity a single cone on a perfectly conducting plane is drawn. The even modes are also included, whereas for the biconical antenna only the odd modes occur. Each mode was represented by one electric line loop. To avoid confusion the loops were drawn successively towards the center of the picture. However, they should be imagined as "stacked" upon each other near the imaginary boundary shpere, since it is there that the interior modes are transformed to the exterior modes as the energy propagates from the center outwards.

An examination of the above picture shows that for infinitesimally thin cones the respective mode loops of both regions approach each other in size. Since modes of one region show maximum coupling to similar modes of an adjacent region, and in limiting cases where the regions become identical the modes must also become identical, it is readily seen that for infinitesimally thin biconical antennas each interior mode will couple only to the same exterior

---

*The dashed line represents an electric line of force for the interior dominant mode.

mode. That this is the case will be shown in the next section, where it is proved that in the limit as $\theta_o \rightarrow 0^o$ the interior mode coefficients a_n become equal to the exterior mode coefficients b_m.

For thick cones the various modes for the two regions can be pictured as follows:

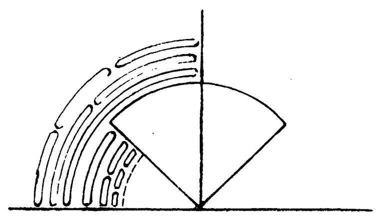

FIGURE 4. MODE REPRESENTATION FOR THICK CONES

A comparison of the loop sizes in the two regions shows maximum coupling between the largest inside mode (one loop) and the third outside mode (three loops).

For very thick cones the mode coupling picture suggests little coupling between the low exterior modes and the interior modes.

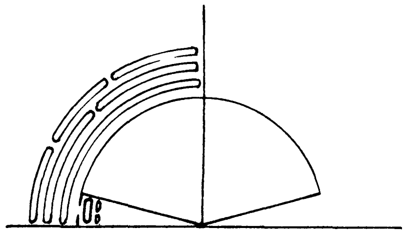

FIGURE 5. ELECTRIC LINES FOR VERY THICK CONES

As the cone angle θ_0 approaches 90^o, the coupling of the exterior modes to the interior modes vanishes. Only the TEM mode exists in the infinitesimally thin slit (or ring source) around the sphere and couples to all exterior modes. In this case the TEM mode can go beyond the ficitious mathematical boundary (as opposed to the case of the very thin cone) as shown in the following figure:

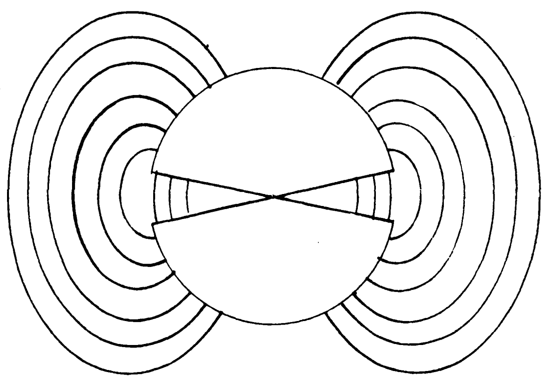

FIGURE 6. ELECTRIC LINES OF THE TEM MODE
ON THE VERY THICK BICONICAL ANTENNA

Another way to represent mode coupling is to indicate along two parallel lines the order of the modes. Table I gives the mode index n_i of the interior modes for different cone angles. The exterior mode indices are the odd numbers r. The graphs are plotted in Figure 7.

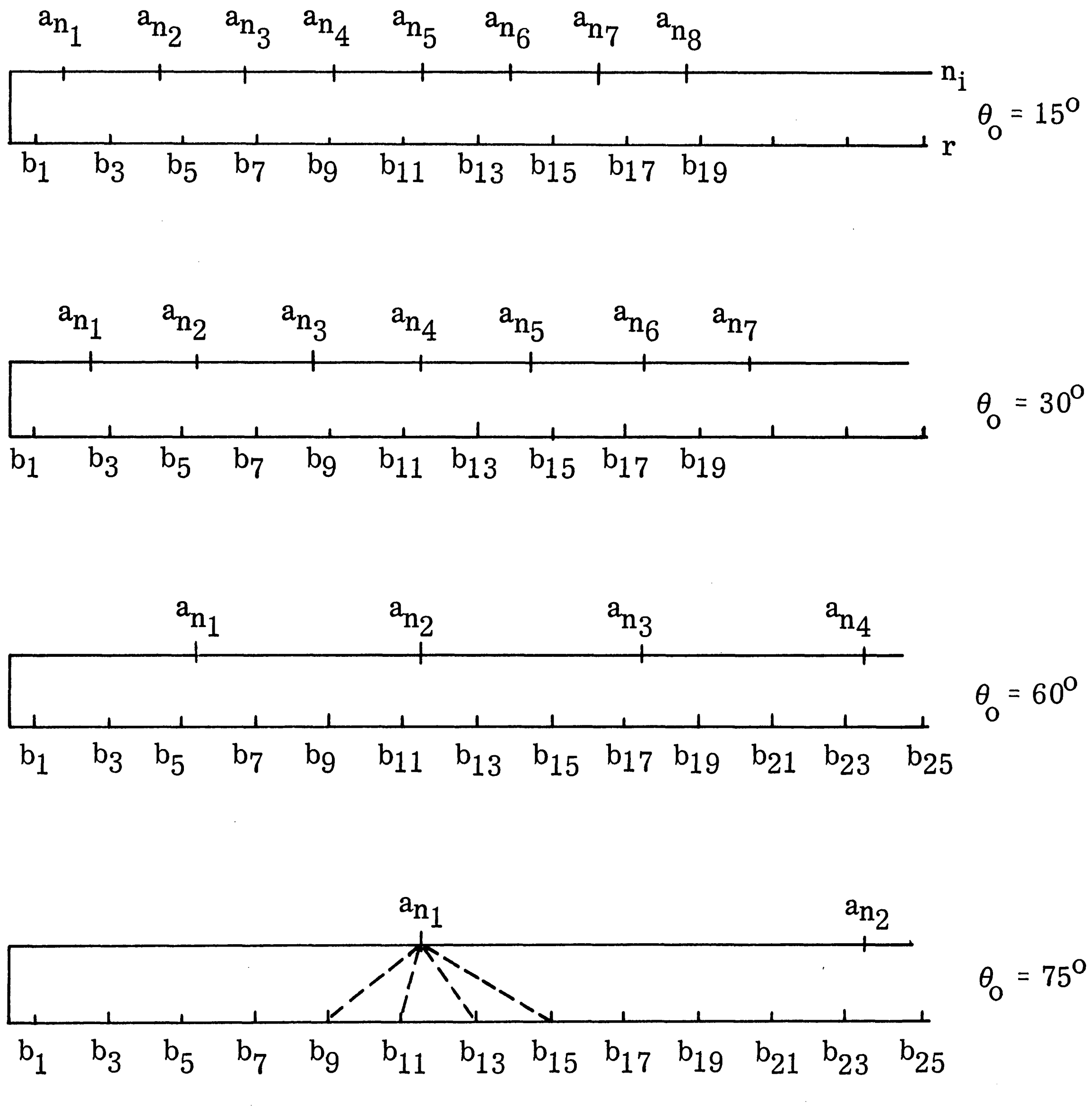

FIGURE 7. MODE INDICES OF THE TWO REGIONS DRAWN TO DISPLAY MODE COUPLING

Equation (II-5), which gives the expansion of one interior mode coefficient a_{n_i} in terms of all the exterior mode coefficients b_m, shows that the factor $\frac{1}{n_i - m}$ will select a set of preferred exterior modes which are dominant in the expansion. To show this dependence explicitly one can write

$$a_{n_i} = F\left(\frac{b_m}{m - n_i}\right) \tag{VIII-1}$$

Thus the most preferred exterior mode (or the dominant one) is given when the summation index m is closest in numerical value to n_i. The preferred, finite mode set, hereafter called the subset is determined by a few values of m on either side of n_i.

Similarly equation (II-6) which states the expansion of one exterior mode coefficient b_m in terms of all the interior mode coefficients a_{n_i} can be written as

$$b_m = \text{TEM} + f\left(\frac{a_{n_i}}{n_i - m}\right) \tag{VIII-2}$$

Figure 7 displays this coupling of one mode in a region to a subset of modes in the other region. For example, the last graph shows that maximum coupling exists between the a_{n_1} and the b_{11} mode, and that it would not be unreasonable to represent a_{n_1} accurately by the few exterior modes which have maximum coupling to a_{n_1} (the dotted lines define a preferred mode set).

The behavior of the two limiting cases when $\theta_o \rightarrow 0^o$ and $\theta_o \rightarrow 90^o$ can be easily deduced. For thin cones the interior modes approach the respective exterior modes. In the limit as $\theta_o \rightarrow 0^o$, the interior mode index $n_i \rightarrow m$, and thus the factor $\frac{1}{n_i - m}$ selects only one mode, i.e., cross coupling exists between like modes only. For very thick cones the interior mode indices become very large with the result that only a few interior modes have to be included in the expansion of one exterior mode coefficient. In the limit as $\theta_o \rightarrow 90^o$, the values of n_i become infinitely large, leaving only the TEM mode in the interior region to couple to all the exterior modes.

IX

EXACT SOLUTION FOR THIN AND THICK CONES

A. Exact Solution When The Cone Angle $\theta_o \to 0^o$.

There are two special limiting cases for which the mode coefficients b_r are known exactly. One, when the cone angle $\theta_o \to 0^o$ and the other when $\theta_o \to 90^o$. Both of these cases have been considered by Schelkunoff [1]. Perhaps the easiest way to derive these is to start with the set of simultaneous infinite equations for b_r, equation (II-10). The roots n_i as $\theta_o \to 0^o$ are given by [1]

$$n_i = r + \frac{1}{\log \frac{2}{\theta_o}}, \quad r = 1, 3, 5, \ldots, \tag{IX-1}$$

i.e. n_i approaches the odd integers as $\theta_o \to 0^o$. The term $\sin\theta_o \frac{dn}{d\theta_o}$ in equation (II-10) can then be expressed:

$$\sin\theta_o \frac{dn}{d\theta_o} = (n-r)^2 = \left(\frac{1}{\log \frac{2}{\theta_o}}\right)^2 \tag{IX-2}$$

and writing the factors in the denominator of equation (II-10) as

$$r(r+1) - n(n+1) = (r-n)(r+n+1),$$

these, for $\theta_o \to 0^o$, can then be written as

$$\lim_{n \to r} (r-n)(r+n+1) = (r-n)(2r+1) \tag{IX-3}$$

With these preliminaries the term under the double summation sign in equation (II-10) takes on the following form

$$\lim_{\theta_0 \to 0} \frac{\sin\theta_0 \; dn/d\theta_0}{\left[r(r+1)-n(n+1)\right]\left[m(m+1)-n(n+1)\right]} = \begin{cases} 0, & m \neq r \neq n \\ \dfrac{1}{(2r+1)^2}, & m = r = n \end{cases} \qquad \text{(IX-4)}$$

Thus equation (II-10) for infinitesimally thin cones, using the relation

$$\lim_{\theta_0 \to 0} P_r(\cos\theta_0) = 1$$

becomes

$$i + \frac{1}{2r+1}\frac{R'_r}{R_r} b_r = r(r+1)\, b_r \frac{2r+1}{r(r+1)} \frac{S'_r}{S_r} \frac{1}{(2r+1)^2} \qquad \text{(IX-5)}$$

or

$$b_r = \frac{i(2r+1)\, R_r\, S_r}{S'_r R_r - R'_r S_r}. \qquad \text{(IX-6)}$$

The dominator of the above expression is the Wronskian equation (VII-17). Using its value the exterior mode coefficients b_r for infinitesimally thin biconical antennas are then given by

$$b_r = \frac{\pi}{2}\,(2r+1)\, R_r\, S_r \qquad \text{(IX-7)}$$

or using the definitions of R_r and S_r (equations II-8, II-9)

$$b_r = \frac{\pi}{2} k\ell (2r+1) J_{r+1/2} (k\ell) H^{(2)}_{r+1/2} (k\ell) \qquad \text{(IX-8)}$$

and the load admittance

$$Y_L = \frac{120}{Z_o^2} \sum_{r=1,3}^{\infty} \frac{b_r P_r(\cos\theta_o)}{r(r+1)} \qquad \text{(II-11)}$$

becomes

$$Y_L = \frac{120}{Z_o^2} \frac{\pi}{2} k\ell \sum_{r=1,3}^{\infty} \frac{2r+1}{r(r+1)} J_{r+1/2} (k\ell) H^{(2)}_{r+1/2} (k\ell) \qquad \text{(IX-9)}$$

In the physical picture, as the cone angle $\theta_o \rightarrow 0^o$, the modes decouple, i.e., the interior and exterior mode coefficients become equal ($a_n = b_m$) and all that is left is to crossmatch modes of like order in the two regions. Cross-coupling between different modes shows its effect only as a perturbation which dies out as $\theta_o \rightarrow 0^o$. Mathematically, the matrix for b_r decouples, i.e., only the diagonal terms of the matrix remain. Again, the off-diagonal terms contribute only as perturbation terms which vanish as $\theta_o \rightarrow 0^o$. When the cone angle becomes larger than zero but still very small, the terms closest to the diagonal of the matrix will begin to couple to the diagonal terms, and as the cone angle gets larger, more off-diagonal terms will come into play. Usable results for cone angles as large as 30^o can be obtained by simplifying the original matrix (equation II-10) to a super-diagonal matrix consisting of the diagonal terms and one term each side of the diagonal. This super-diagonal matrix can be expressed with the help of equation (VII-1), which is an abbreviated form of equation (II-10), as

$$B_r = \sum_{m=r-2}^{r+2} (I_r^m - \delta_{rm})\, b_m \tag{IX-10}$$

where δ_{rm} is the Kronecker delta.

B. A Solution for Thin Cones.

It was concluded in the previous section that the coupling between like modes of the interior and exterior region becomes stronger as the cone angle becomes smaller. This can be directly expressed (from equation VII-1) by

$$\lim_{\theta_0 \to 0^o} \sum_m I_r^m\, b_m \to I_r^r\, b_r\ .$$

Thus, for cones whose angle is small, but not zero, the diagonal terms alone are a good approximation to the coefficients b_r. Using equation (VII-1), this can be expressed as

$$b_r = \frac{B_r}{1 - I_r^r} \tag{IX-11}$$

Instead of going to the limit ($\theta_o \to 0^o$), as was done in the previous section, the i-sum which is contained in the diagonal terms (see equation VI-2) I_r^r will be further simplified, appropriate for small cone angles. The physical interpretation of this is that each exterior mode is given by only one interior mode, namely that interior mode which is closest to the exterior mode (being considered) in index number. That this is exactly what happens for infinitesimally small cones was shown in the previous section; for thin cones this should be a valid approximation. Thus b_r can be written explicitly from equation (II-10), or equation (V-1) as

$$b_r = \frac{-i\, P_r\,(2r+1)\,\dfrac{R_r}{R_r'}}{1 - \dfrac{r(r+1)(2r+1)(2n^{(r)}+1)\,P_r^2}{n^{(r)}(n^{(r)}+1)\left[r(r+1) - n^{(r)}(n^{(r)}+1)\right]^2}\,\sin\theta_o\,\dfrac{dn^{(r)}}{d\theta_o}\,\dfrac{S'_{n^{(r)}}}{S_{n^{(r)}}}\,\dfrac{R_r}{R_r'}} \qquad \text{(IX-12)}$$

where $n^{(r)}$ is that root n_i which is closest to r. When the limit, as $\theta_o \to 0^o$, is applied to the above expression the correct expression for infinitesimally thin equation (IX-6) is obtained.

C. Exact Solution When the Cone Angle $\theta_o \to \pi/2$.

The second limiting case for which the mode coefficients b_r are known exactly is when the cone angle $\theta_o \to \pi/2$. It is seen from equation (III-2) that the roots n_i, as $\theta_o \to \pi/2$, approach infinity. In chapter V, equation (V-4), it was shown that the i-sum vanishes as $n_i \rightarrow \infty$. Thus in the matrix for b_r, equation (VII-1), which reads

$$b_r = B_r + \sum_m I_r^m b_m \qquad \text{(VII-1)}$$

the term I_r^m contains the i-sum (see equation VII-4 or equation V-1) and therefore goes to zero when $\theta_o \rightarrow \pi/2$. Thus

$$\lim_{\theta_o \rightarrow \pi/2} b_r = B_r \qquad \text{(IX-13)}$$

or using the definition of B_r, equation (VII-2)

$$\lim_{\theta_o \rightarrow \pi/2} b_r = - i\, P_r \,(2r + 1)\, \frac{R_r}{R'_r}$$

and the load admittance as the cone angle approaches 90^o is then

$$Y_L = \frac{120}{i\, Z_o^2} \sum_{r=1}^{\infty} \frac{2r + 1}{r(r+1)} \, \frac{R_r\,(k\ell)}{R'_r\,(k\ell)} \, P_r^2\,(\cos\theta_o) \qquad \text{(IX-14)}$$

In conclusion one can say that for this limiting case all the interior modes except the dominant mode vanish. The exterior mode coefficients b_r are then given by (or matched to) the TEM mode only, as expressed by equation (IX-13). This becomes even more apparent when the expression for one exterior mode in terms of the TEM and all interior modes is examined. Equation (II-6) gives this relationship and can be written as follows

$$b_r = -i P_r (2r+1) \frac{R_r}{R'_r} \left(1 + i\, r(r+1) \sum_{i=1}^{\infty} \frac{a_{n_i}}{n_i(n_i+1)} \frac{\sin\theta_o}{n_i(n_i+1) - r(r+1)} \frac{S'_{n_i}}{S_{n_i}} \frac{\partial L_{n_i}}{\partial \theta_o}\right) \tag{II-6}$$

The i-sum, which represents all the higher interior modes, vanishes as $n_i \to \infty$. Thus b_r is given by the factor outside the parenthesis which represents the TEM mode and is equal to (IX-13).

Unlike the expression for infinitesimally thin cones, the expression derived for the 90^o cones is also a good approximation for thick cones. It can be used to calculate the coefficients for cones as "thin" as 60^o with good accuracy. This is also concluded in a report by Papas and King [2] and in a paper by Smith [3]. Smith, however, states optimistically that this expression (equation IX-13) can be applied to cones whose angle exceeds 39.2^o if rough results are required. If indeed only rough results are desired the expression for the load admittance, equation (IX-14), can be further simplified. In Section V it was pointed out that the first few modes were the most important ones in a calculation for the load admittance. For rough results then the sum in the above expression can be approximated by its first term, thus

$$Y_L \approx \frac{180}{i Z_o^2} \frac{R_1(k\ell)}{R'_1(k\ell)} P_1(\cos\theta_o) \tag{IX-15}$$

However the use of this equation should be restricted to large cone angles.

D. A Solution for Thick Cones.

The graphs of Figure 7 display the vanishing of the higher order interior modes for very thick cones. Based upon this observation one can say that for thick cones a more accurate expression for the mode coefficients b_r can be obtained by matching the exterior modes to the dominant mode and one interior mode. For example, the graph for $\theta_o = 75^o$, in Figure 7 shows that the first seven coefficients of b could best be represented by the first interior mode a_{n_1} and the TEM mode. Thus from equation (II-6), page 47, it follows that for thick cones

$$b_r = i P_r (2r+1) \frac{R_r}{R'_r} \left(1 - i \frac{r(r+1)}{n_1(n_1+1)} \frac{\sin\theta_o}{r(r+1) - n_1(n_1+1)} \frac{S'_{n_1}}{S_{n_1}} \frac{\partial L_{n_1}}{\partial \theta_o} a_{n_1}\right) \tag{IX-16}$$

substituting this expression for b_r in equation (II-5)

$$a_{n_1} = \frac{2n_1 + 1}{\frac{\partial L_{n_1}}{\partial n_1}} \sum_{m=1}^{\infty} \frac{-i(2m+1)\, P_m^2}{m(m+1) - n_1(n_1+1)} \frac{R_m}{R'_m} \cdot$$

$$\cdot \left(1 - i \frac{m(m+1)}{n_1(n_1+1)} \frac{\sin\theta_o}{m(m+1) - n_1(n_1+1)} \frac{S'_{n_1}}{S_{n_1}} \frac{\partial L_{n_1}}{\partial \theta_o} a_{n_1}\right)$$

(IX-17)

this can be solved now for the first internal mode coefficient a_{n_1}. With a_{n_1} known, equation (IX-16) yields the corrected mode coefficients for thick cones. Thus,

$$b_r = -i P_r (2r+1) \frac{R_r}{R'_r} \left(1 - \frac{r(r+1)}{n_1(n_1+1)} \frac{2n_1+1}{n_1(n_1+1) - r(r+1)} \sin\theta_o \frac{dn_1}{d\theta_o} \frac{S'_{n_1}}{S_{n_1}} \cdot\right.$$

$$\left. \cdot \frac{\displaystyle\sum_{m=1}^{\infty} \frac{2m+1}{m(m+1) - n_1(n_1+1)} P_m^2 \frac{R_m}{R'_m}}{\displaystyle 1 - \frac{2n_1+1}{n_1(n_1+1)} \sin\theta_o \frac{dn_1}{d\theta_o} \frac{S'_{n_1}}{S_{n_1}} \sum_{m=1}^{\infty} \frac{m(m+1)(2m+1)}{\left(m(m+1) - n_1(n_1+1)\right)^2} P_m^2 \frac{R_m}{R'_m}}\right)$$

(IX-18)

This shows the complexity of the correction term, obtained by including one interior mode. The term multiplying the parenthesis is, of course, just the contribution of the TEM mode as given by equation (IX-13) or by omitting all the interior modes in equation (II-6).

The exterior mode coefficients can still be obtained more accurately by including two interior modes instead of only one. The added accuracy gained might not be as important as the validity of such an expression to be used for even "thinner" cones. That this is the case is shown by the graphs of Figure 7: the thinner the cones are the more interior modes must be included. Such a correction would not be difficult to carry out. Equation (IX-16) would be replaced by an expression with two interior modes a_{n_1} and a_{n_2}. This would yield two simultaneous equations for a_{n_1} and a_{n_2} in place of equation (IX-17). Solving these two equations and substituting the solutions in the equivalent of equation (IX-16) completes the procedure. Accurate results from such an expression can be expected for at least the first three exterior mode coefficients for cones as thin as 30^{o}, as borne out by the second graph in Figure 7.

Some terms in the above expression can be simplified, considering that equation (IX-18) is valid for thick cone angles, for example the term

$$\frac{2n_1 + 1}{n_1(n_1 + 1)} \frac{dn_1}{d\theta_o} \frac{S'_{n_1}}{S_{n_1}} \approx \frac{2}{\pi k \ell} \frac{\rho^3}{\rho^2 - 1/4} (\rho - 1/2) \qquad \text{(IX-19)}$$

To derive the above result, equations (III-2), (III-3), (IV-5), and (VI-10) have been used.

E. An Approximation for Any Cone Angle

The method of Section D can be extended to give an approximate solution for any cone angle. The crudest approximation is obtained when any b_r is approximated by one coefficient a_{n_i}. This is similar to equation (IX-16), except that now n_1 is replaced by that n_i which is closest in numerical value to r, i. e. the dominant coefficient a_{n_i} is selected. The solution for any b_r is then given by equation (IX-18). For better accuracy b_r can be approximated by two coefficients a_{n_i}. The n_i's are again chosen to be nearest to r. This can be illustrated using a condensed notation for b_r and a_{n_i}, i. e.

$$b_r = B_r + \sum_i (r, n_i)\, a_{n_i} \qquad \text{(IX-20)}$$

$$a_{n_i} = \sum_m \langle m, n_i \rangle\, b_m \qquad \text{(IX-21)}$$

where the b_r's and a_{n_i}'s are written out explicitly in equations (II-6) and (II-5) respectively. Approximating b_r by two a_{n_i}'s

$$b_r \approx B_r + (r, n_i)\, a_{n_i} + (r, n_{i+1})\, a_{n_{i+1}} \qquad \text{(IX-22)}$$

where n_i is closest in numerical value to r and n_{i+1} is next closest. For example, from Figure 7 in the graph for $\theta_o = 60^o$, b_1 should be approximated by a_{n_1} and a_{n_2} and b_{17} by a_{n_2} and a_{n_3}. The two coefficients a_{n_i} and $a_{n_{i+1}}$ can now be found by substituting b_r from equation (IX-22) into equation (IX-21) for a_{n_i}. Thus,

$$a_{n_i} = \sum_m \langle m, n_i \rangle B_m + \sum_m \langle m, n_i \rangle (m, n_i) a_{n_i} + \sum_m \langle m, n_i \rangle (m, n_{i+1}) a_{n_{i+1}}$$

(IX-23)

$$a_{n_{i+1}} = \sum_m \langle m, n_{i+1} \rangle B_m + \sum_m \langle m, n_{i+1} \rangle (m, n_i) a_{n_i} + \sum_m \langle m, n_{i+1} \rangle (m, n_{i+1}) a_{n_{i+1}}.$$

(IX-24)

This system has the solution

$$a_{n_i} = \frac{\left(\sum_m \langle m,n_{i+1} \rangle B_m\right)\left(\sum_m \langle m,n_i \rangle (m,n_{i+1})\right) - \left(\sum_m \langle m,n_i \rangle B_m\right)\left(\sum_m \langle m,n_{i+1} \rangle (m,n_{i+1}) -1\right)}{\left(\sum_m \langle m,n_i \rangle (m,n_i) -1\right)\left(\sum_m \langle m,n_{i+1} \rangle (m,n_{i+1}) -1\right) - \left(\sum_m \langle m,n_{i+1} \rangle (m,n_i)\right)\left(\sum_m \langle m,n_i \rangle (m,n_{i+1})\right)}.$$

(IX-25)

The solution for $a_{n_{i+1}}$ is similar except that n_i and n_{i+1} are interchanged. The two coefficients a_{n_i} and $a_{n_{i+1}}$ can now be substituted into the expression for b_r, equation (IX-22), to give any exterior mode coefficient. The approximation can be continuously improved by including more and more coefficients of lesser singificance in the approximation for b_r. It is interesting to note that this method of approximation gives better accuracy for the first few b_r's, especially b_1. This can be easily seen from Figure 7. The coefficient b_1, especially for larger cone angles, is better approximated by a_{n_1} and a_{n_2} then say b_{17} is by a_{n_1} and a_{n_2} (for $\theta_o = 75^o$

on Figure 7). This improved accuracy is very desireable since the expression for the load admittance Y_L, equation (V-8), depends mostly on b_1.

The success of this method depends largely upon how readily sums such as

$$\sum_m \langle m, n_i \rangle B_m = \frac{2n_i + 1}{\dfrac{\partial L_{n_i}}{\partial n_i}} \sum_m \frac{-i(2m+1)\, P_m^2}{m(m+1) - n_i(n_i+1)} \; \frac{R_m}{R'_m}$$

which occur in the solutions for a_{n_i} can be calculated.

X

SOLUTION FOR THE EXTERIOR MODE COEFFICIENTS b USING A FINITE SET OF PREFERRED MODES

The infinite simultaneous equations for b_r represent mathematically the interaction of all interior modes with all exterior modes. For special cone angles the interaction between the modes simplifies greatly. It was shown in a previous section, that for small-angle cones only the coupling between modes of nearly the same order is significant whereas for large-angle cones interaction between the TEM mode and all exterior modes exists. In the set of simultaneous equations

$$b_r = B_r + \sum_m I_r^m \, b_m$$

the term I_r^m gives the relationship between the modes. It can be written as

$$I_r^m = i_r^n \, i_n^m$$

where

i_r^n relates coupling from the r^{th} exterior mode to the n^{th} interior mode

i_n^m relates coupling from the n^{th} interior mode to the m^{th} exterior mode.

The development of a relatively simple approximate solution for arbitrary cones depends largely on what approximations can be made in the term I_r^m. A clue is provided by the two limiting cases. There, the relatively simple expressions were obtained by observing that not all modes of both regions play an equally important part in matching the fields across the boundary.

A similar reduction in modes for thick cones takes place when only modes which show maximum coupling to a mode of the other region are included in the matching of fields. Using only a finite set of modes, the subset instead of an infinity of modes should result in a singificant simplification.

The concept of a finite, preferred mode set which was already discussed in Section VIII is more apparent when the expressions for the modes in place of the infinite matrix are examined. Thus,

$$a_{n_i} = \frac{2n_i + 1}{\dfrac{\partial L_{n_i}}{\partial n_i}} \sum_{m=1}^{\infty} \frac{P_m b_m}{m(m+1) - n_i(n_i+1)} \tag{II-5}$$

and

$$b_r = - i(2r+1) P_r \frac{R_r}{R'_r} \left(1 + ir(r+1) \sum_{i=1}^{\infty} \frac{a_{n_i}}{n_i(n_i+1)} \; \frac{\sin\theta_o}{n_i(n_i+1) - r(r+1)} \; \frac{S'_{n_i}}{S_{n_i}} \; \frac{\partial L_{n_i}}{\partial \theta_o}\right) \tag{II-6}$$

In equation (II-5) a term exists which is dominant in the series. This term occurs in the summation when the integer m is closest in numerical value to n_i, thus let

$$m = n_i + \Delta_i \tag{X-1}$$

where Δ_i is a fraction, when added to n_i gives the nearest odd integer. That being the case the denominator can be expressed as

$$m(m+1) - n_i(n_i+1) = \Delta_i\,(2n_i + 1 + \Delta_i) \tag{X-2}$$

Approximating a_{n_i} by this dominant term we can write

$$a_{n_i} \approx \frac{2n_i + 1}{\dfrac{\partial L_{n_i}}{\partial n_i}} \; \frac{P_{n_i+\Delta_i}\, b_{n_i+\Delta_i}}{\Delta_i(2n_i + 1 + \Delta_i)} \tag{X-3}$$

This can now be substituted in the expression for b_r to give

$$b_r = -\,i(2r+1)\,P_r\,\frac{R_r}{R'_r}\left(1 + ir(r+1)\sum_{i=1}^{\infty}\frac{2n+1}{n_i(n_i+1)}\,\frac{\sin\theta_o\,P_{n_i+\Delta_i}\,b_{n_i+\Delta_i}}{\Delta_i(2n_i+1+\Delta_i)\big(r(r+1)-n_i(n_i+1)\big)}\,\frac{dn_i}{d\theta_o}\cdot\frac{S'_{n_i}}{S_{n_i}}\right) \tag{X-4}$$

where

$$\frac{\partial L_{n_i}}{\partial \theta_o} \bigg/ \frac{\partial L_{n_i}}{\partial n_i} = -\,\frac{dn_i}{d\theta_o}$$

The above expression can be interpreted as relating any exterior mode b_r to some selected modes $b_{n_i+\Delta_i}$ which show strong coupling to the interior modes. Now to determine $b_{n_i+\Delta_i}$ one observes that it is well approximated by one interior mode (in equation II-6) which has its index number near $n_i + \Delta_i$ and is, of course, the a_{n_i} mode. Perhpas this can be best seen from the last graph in Figure 7. According to this graph, a_{n_1} in equation (X-3) would be best approximated by b_{11} and in turn b_{11} by a_{n_1}. Such a procedure selects a group of paired modes, one from the interior and the other from the exterior region which show maximum coupling to each other. It will be possible to solve for these modes explicity. After their solution is known they are employed in equation (X-4) to obtain any unknown mode b_r. In the case of infinitesimally thin cones, strong coupling exists for all the modes. For such thin cones any mode from the interior regions couples to only one other mode of the exterior region. Pairing such modes of maxiumum coupling will then lead to the exact solution. This notion is made use of here, where for thick cones some modes show a similar strong coupling to one other mode. Proceeding, $b_{n_i+\Delta_i}$ is then given by

$$b_{n_i+\Delta_i} = -i\left(2(n_i+\Delta_i)+1\right) P_{n_i+\Delta_i} \frac{R_{n_i+\Delta_i}}{R'_{n_i+\Delta_i}} \cdot$$

$$\left(1 + \frac{i\, a_{n_i}}{n_i(n_i+1)} \; \frac{\sin\theta_0\,(n_i+\Delta_i)(n_i+\Delta_i+1)}{n_i(n_i+1)-(n_i+\Delta_i)(n_i+\Delta_i+1)} \; \frac{S'_{n_i}}{S_{n_i}} \; \frac{\partial L_{n_i}}{\partial\theta_o}\right) \tag{X-5}$$

Substituting a_{n_i} from equation (X-3) and solving for the selected modes $b_{n_i+\Delta_i}$

$$b_{n_i+\Delta_i} = -i\left(2(n_i+\Delta_i)+1\right) P_{n_i+\Delta_i} \frac{R_{n_i+\Delta_i}}{R'_{n_i+\Delta_i}} \left(1 - \left(2(n_i+\Delta_i)+1\right) P_{n_i+\Delta_i} \frac{R_{n_i+\Delta_i}}{R'_{n_i+\Delta_i}} \cdot\right.$$

$$\left. \cdot \frac{2n_i+1}{n_i(n_i+1)} \frac{\sin\theta_o (n_i+\Delta_i)(n_i+\Delta_i+1)}{\Delta_i^2 (2n_i+1+\Delta_i)^2} \frac{dn_i}{d\theta_o} \frac{S'_{n_i}}{S_{n_i}}\right)^{-1} \qquad \text{(X-6)}$$

This can now be used in equation (X-4) above. The approximate solution for the exterior mode coefficients b_r is then

$$b_r = -i(2r+1) P_r \frac{R_r}{R'_r} \left[1 + r(r+1) \sum_{i=1}^{\infty} \frac{2n_i+1}{n_i(n_i+1)} \frac{\sin\theta_o \left(2(n_i+\Delta_i)+1\right) P^2_{n_i+\Delta_i}}{\Delta_i(2n_i+1+\Delta_i)\left(r(r+1)-n_i(n_i+1)\right)} \frac{dn_i}{d\theta_o} \frac{S'_{n_i}}{S_{n_i}} \cdot\right.$$

$$\cdot \frac{R_{n_i+\Delta_i}}{R'_{n_i+\Delta_i}} \left(1 - \left(2(n_i+\Delta_i)+1\right) P_{n_i+\Delta_i} \frac{R_{n_i+\Delta_i}}{R'_{n_i+\Delta_i}} \frac{2n_i+1}{n_i(n_i+1)} \cdot\right.$$

$$\left.\left. \cdot \frac{\sin\theta_o (n_i+\Delta_i)(n_i+\Delta_i+1)}{\Delta_i^2 (2n_i+1+\Delta_i)^2} \frac{dn_i}{d\theta_o} \frac{S'_{n_i}}{S_{n_i}}\right)^{-1}\right] \qquad \text{(X-7)}$$

To illustrate the use of the Δ's in the above expression let us choose a 60-degree cone and calculate some values of Δ_i with the help of Table I. In general for such thick cones the above summation will show rapid convergence and the first few terms of the series should be a good approximation. For the first four values of

n_i (5.48, 11.489, 17.493, 23.494) the nearest corresponding odd integers are 5, 11, 17, and 23. Thus equation (X-1) would give the first four Δ's as -.48, -.489, -.493, and -.494.

In Section VII it was concluded that for thin cones the convergence of a series developed from an expression like equation (X-4) can be greatly improved by combining the diagonal terms with the left side of the equation, i.e. in equation (X-4), the term for which $n_i + \Delta_i = r$ are combined with b_r on the left side. The remaining summation with the $n_i + \Delta_i = r$ term omitted is then designated by a primed summation index i'. When this is applied to equation (X-7) the approximate expression for b_r which is now more accurate for thin cones reads

$$b_r = \frac{-i(2r+1)P_r \dfrac{R_r}{R'_r}\left[1 + r(r+1)\displaystyle\sum_{i'=1}^{\infty} (\text{same as terms in equation X-7})\right]}{1 - r(r+1)(2r+1)P_r^2 \dfrac{R_r}{R'_r}\displaystyle\sum_{i=1}^{\infty} \dfrac{2n_i+1}{n_i(n_i+1)} \dfrac{\sin\theta_0}{\left(r(r+1) - n_i(n_i+1)\right)^2} \dfrac{dn_i}{d\theta_0} \dfrac{S'_{n_i}}{S_{n_i}}} \tag{X-8}$$

The above two expressions are very complicated, considering that only one term was included in the subset. However, if the accuracy of this method is to be increased, more terms must be retained in the subset. A logical step if more accuracy is desired would be to approximate a_{n_i} of equation (X-3) by the dominant term and one term of lesser significance, i.e.

$$a_{n_i} = \frac{2n_i + 1}{\dfrac{\partial L_{n_i}}{\partial n_i}} \left(\frac{P_{n_i+\gamma_i}\, b_{n_i+\gamma_i}}{\gamma_i (2n_i + 1 + \gamma_i)} + \frac{P_{n_i+\Delta_i}\, b_{n_i+\Delta_i}}{\Delta_i (2n_i + 1 + \Delta_i)} \right) \tag{X-9}$$

where

$$m = n_i + \gamma_i \tag{X-10}$$

and γ_i is a number which, when added to n_i, gives the second nearest odd integer m. For example, the last graph of Figure 7 shows that the nearest exterior mode to a_{n_1} is b_{11}, and the second nearest b_{13}. Then with the aid of Table I ($\theta_o = 75^o$)

$$\Delta_1 = 11 - 11.489$$

$$\gamma_1 = 13 - 11.489$$

Similarly, in place of equation (X-4), b_r is given now by

$$b_r = -i(2r+1) P_r \frac{R_r}{R'_r} \left(1 + ir(r+1) \sum_{i=1}^{\infty} \left(\frac{P_{n_i+\gamma_i}\, b_{n_i+\gamma_i}}{\gamma_i (2n_i + 1 + \gamma_i)} + \frac{P_{n_i+\Delta_i}\, b_{n_i+\Delta_i}}{\Delta_i (2n_i + 1 + \Delta_i)} \right) \right.$$

$$\left. \cdot \frac{\sin\theta_o\, (2n_i + 1)}{n_i(n_i+1)\big(r(r+1) - n_i(n_i+1)\big)} \frac{dn_i}{d\theta_o} \frac{S'_{n_i}}{S_{n_i}} \right) \tag{X-11}$$

However expression (X-5), a simple equation in one unknown, is now replaced by two equations in the two unknowns $b_{n_i+\Delta_i}$ and $b_{n_i+\gamma_i}$, where

$$b_{n_i+\Delta_i} = -i\left(2(n_i+\Delta_i)+1\right) P_{n_i+\Delta_i} \frac{R_{n_i+\Delta_i}}{R'_{n_i+\Delta_i}} \left(1 + \frac{i\sin\theta_o (n_i+\Delta_i)(n_i+1+\Delta_i)(2n_i+1)}{n_i(n_i+1)\Delta_i(2n_i+1+\Delta_i)} \cdot \right.$$

$$\left. \cdot \frac{dn_i}{d\theta_o} \frac{S'_{n_i}}{S_{n_i}} \left(\frac{P_{n_i+\gamma_i} b_{n_i+\gamma_i}}{\gamma_i(2n_i+1+\gamma_i)} + \frac{P_{n_i+\Delta_i} b_{n_i+\Delta_i}}{\Delta_i(2n_i+1+\Delta_i)} \right)\right) \qquad \text{(X-12)}$$

$b_{n_i+\gamma_i}$ = same as equation (X-12), with Δ_i and γ_i interchanged

These two equations determine $b_{n_i+\Delta_i}$ and $b_{n_i+\gamma_i}$. Their solutions can then be used in equation (X-11) to determine any exterior mode b_r with greater accuracy than equation (X-7) would yield.

It is now apparent that in this method of approximation progressively better accuracy can be obtained by including more and more terms in the subset. The above steps essentially imply the procedure to follow when solutions with increasing accuracy are to be derived. For example, a better approximation to the exact solution results when three terms are kept in the subset in place of only two. This, however, will also add to the complexity since now a third order matrix will have to be solved. Every additional term that is included to give a better approximation for the selected mode set will result in a higher order matrix. However, this matrix for the terms in the subset need be solved only once, thereafter it can be utilized to calculate the exterior mode coefficients b_r for arbitrary cones.

Of course, both equation (X-7) and (X-8) give the exact solutions for the two limiting cases. In the limit as θ_o approaches zero degrees these two equations yield

$$\lim_{\theta_o \to 0^o} b_r = \frac{\pi}{2} (2r + 1) R_r S_r \qquad \text{same as (IX-7)}$$

and when θ_o approaches ninety degrees they give

$$\lim_{\theta_o \to \frac{\pi}{2}} b_r = - i(2r + 1) P_r \frac{R_r}{R'_r} \qquad \text{same as (IX-13)}$$

XI

OTHER APPROACHES TO THE SOLUTION OF THE BICONICAL ANTENNA

Mathematically the problem of the biconical antenna can be classified as a mixed boundary value problem. Schelkunoff utilized the classical mode theory of transmission lines and wave guides to solve it. Later C. T. Tai derived the variational statement of the problem, and showed that as far as the solution is concerned nothing is gained over Schelkunoff's formulation. J. A. Meier and A. Leitner [11] used functional theoretical techniques to solve the simpler mixed boundary value problem of a hollow, finite biconical sheet antenna. The input impedance was related to an unknown function which was the Lebedev transform of the radial electric field. By omitting the spherical caps on the biconical antenna the boundary conditions were sufficiently relaxed so that the Wiener-Hopf technique was suitable for determining the unknown function. However, no explicit solution was possible, the function was defined by an infinite system of simultaneous equations.

An important contribution was made by C. T. Tai [4] in the variational statement of the biconical antenna problem. An integral equation for the aperture field is first obtained by matching the electromagnetic field along the boundary sphere. Using this integral equation, a function that defines the load admittance of the biconical antenna is expressed in a form which is stationary with respect to the aperture field. Unable to determine the aperture field in closed form an expansion in a complete set of orthogonal functions appropriate to the interior region with unknown coefficients was then made. The coefficients were shown to satisfy an infinite set of linear equations. This set is identical to the infinite matrix for the interior coefficients a_{n_i} which can be obtained by substituting the expression for b_r (equation II-6) in the expression for a_{n_i} (equation II-5). If the aperture field is expanded in terms of the orthogonal functions of the exterior region, an infinite matrix would be derived identical to the one for b_r (equation II-10) used in this study.

The infinite matrix for the mode coefficients is complex and unsymmetric. An attempt to reduce the matrix to diagonal form would first involve a solution for the roots of the characteristic matrix equation. Even if such a solution to the equation of infinite order were possible it would be difficult to attach any meaning to the transformed quantities.

XII

CALCULATION OF THE INPUT AND LOAD IMPEDANCE

The evaluation of the load admittance as given by equations (X-7) and (X-8) was carried out on the IBM-704 computer. Subroutines for the spherical Bessel and Hankel functions S_{n_i} and R_m for arbitrary order and argument were written. The necessary Legendre functions of odd integer order were found tabulated in the literature [12].

The roots n_i for some cone angles are recorded in Table I. A more extensive tabulation of n_i and its derivative calculated from equation (III-11) and (III-12) will now be listed:

TABLE II. THE ROOTS n_i AND THEIR DERIVATIVES

n_i \ θ_o	10^o	15^o	20^o	30^o	40^o	45^o
n_i	1.594	1.795	1.993	2.448	3.063	3.468
n_2	3.908	4.239	4.597	5.470	6.679	7.482
n_3	6.184	6.657	7.182	8.479	10.286	11.488
n_4	8.449	9.066	9.761	11.484	13.889	15.491
n_5	10.708	11.473	12.337	14.487	17.491	19.492
n_6	12.965	13.877	14.911	17.489	21.092	23.494
n_7	15.220	16.280	17.485	20.491	24.693	27.494
n_8	17.473	18.682	20.658	23.492	28.294	31.495

TABLE II. (CONT'D.)

n_i \ θ_o	55^o	60^o	65^o	75^o	80^o	85^o
n_1	4.619	5.480	6.684	11.490	17.493	35.497
n_2	9.773	11.489	13.891	23.495	35.497	71.498
n_3	14.920	17.493	21.094	35.496	53.498	107.499
n_4	20.065	23.494	28.295	47.497	71.498	143.499
n_5	25.209	29.495	35.496	59.498	89.499	179.499
n_6	30.353	35.496	42.697	71.498	107.499	215.499
n_7	35.496	41.497	49.897	83.498	125.499	251.499
n_8	40.639	47.497	57.098	95.497	143.499	287.500

$\sin\theta_o \frac{dn_i}{d\theta_o}$ \ θ_o	10^o	15^o	20^o	30^o	40^o	45^o
i = 1	.444	.589	.810	1.498	2.706	3.652
i = 2	.655	1.015	1.490	2.901	5.332	7.229
i = 3	.907	1.470	2.195	4.332	7.975	10.822
i = 4	1.171	1.934	2.907	5.748	10.622	14.419
i = 5	1.442	2.401	3.621	7.177	13.270	18.017
i = 6	1.715	2.871	4.338	8.607	15.920	21.617
i = 7	1.990	3.343	5.055	10.038	18.570	25.217
i = 8	2.266	3.815	5.773	11.469	21.221	28.817

TABLE II. (CONT'D.)

$\sin\theta_o \frac{dn_i}{d\theta_o}$ \ θ_o	55^o	60^o	65^o	75^o	80^o	85^o
i = 1	6.942	9.968	14.998	44.316	101.61	411.00
i = 2	13.816	19.870	29.932	88.570	203.15	821.94
i = 3	20.705	29.787	44.880	132.84	304.71	1232.89
i = 4	27.598	39.707	59.831	177.11	406.27	1643.85
i = 5	34.492	49.629	74.784	221.38	507.84	2054.81
i = 6	41.386	59.551	89.738	265.66	609.40	2465.76
i = 7	48.282	69.474	104.69	309.93	710.96	2876.72
i = 8	55.177	79.397	119.65	354.20	812.53	3287.68

The results of equation (X-7) and (X-8) will be presented in graphical form. The first pair of graphs shows the real and the imaginary part of the normalized load admittance $Z_o\, Y_L$ which was calculated from equation (V-8).

$$Y_L = \frac{120}{Z_o^2} \cdot \sum_{r=1}^{17} \frac{P_r(\cos\theta_o)}{r(r+1)}\, b_r$$

The remaining graphs display the input impedances of the biconical antenna for various cone angles and lengths. These were obtained from equation (II-13) which is

$$Z_i = Z_o \frac{1 + i\, Z_o Y_L \tan k\ell}{Z_o Y_L + i \tan k\ell}$$

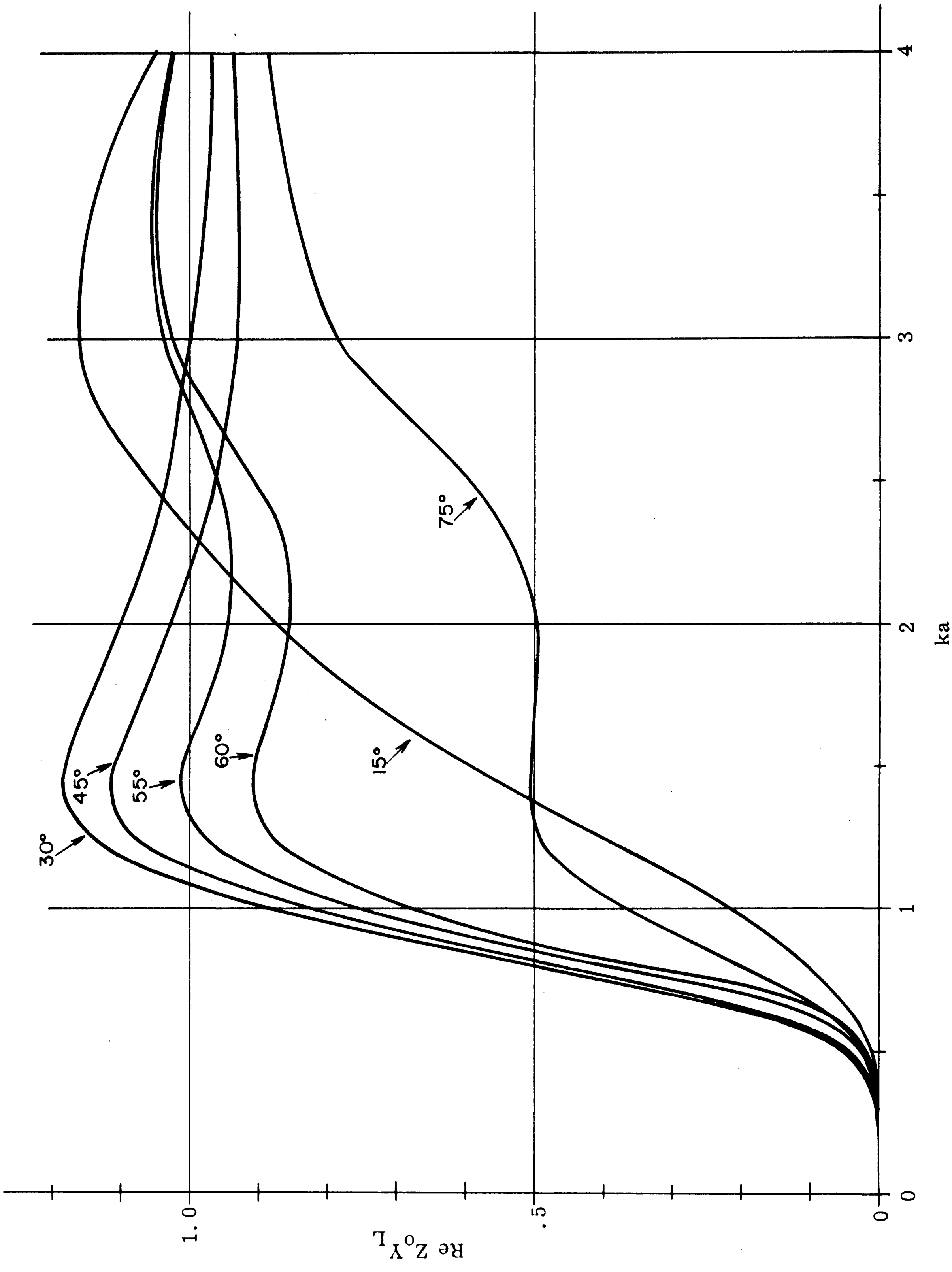

FIGURE 8. THE REAL PART OF THE NORMALIZED LOAD ADMITTANCE AS CALCULATED FROM EQUATION X-7

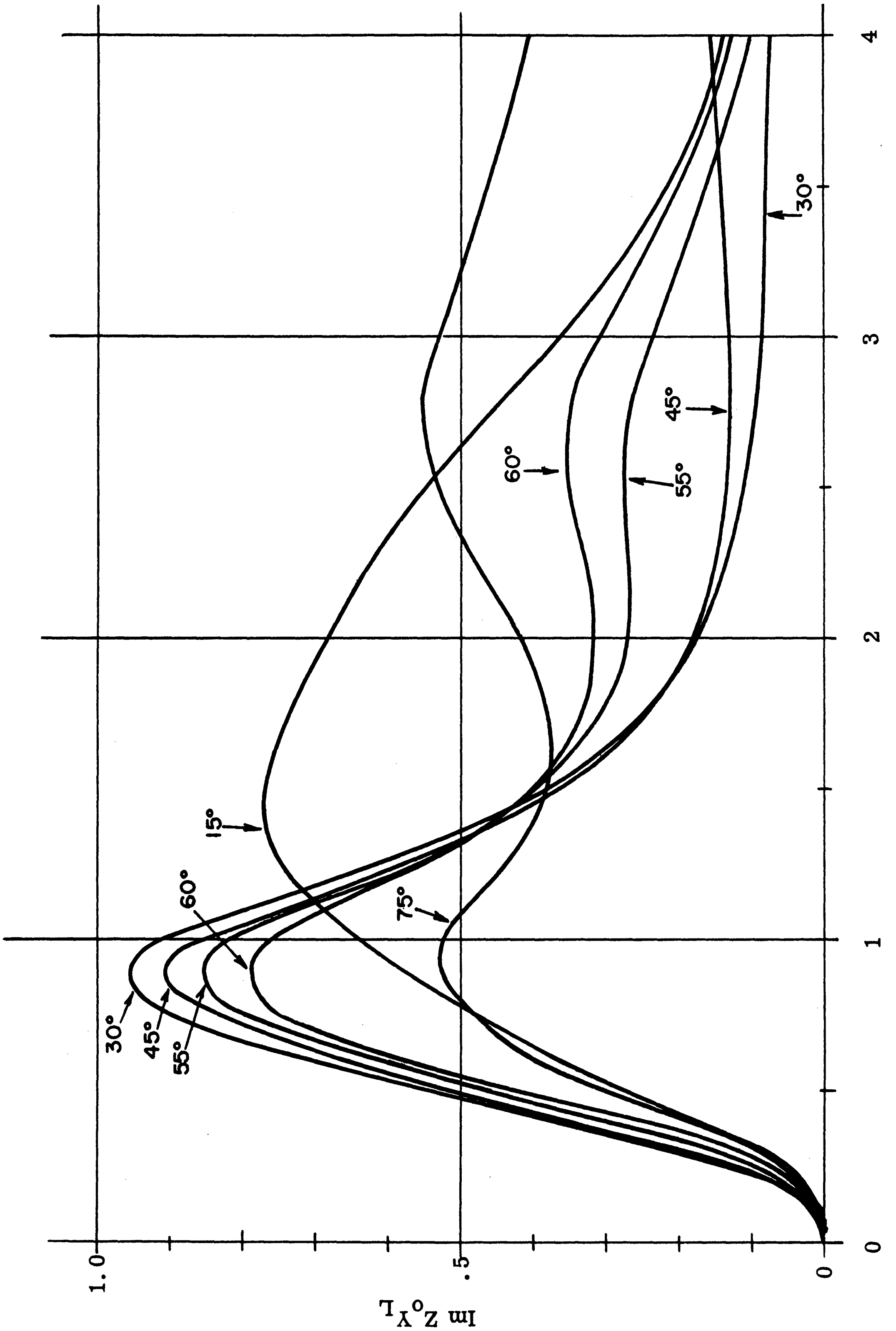

FIGURE 9. THE IMAGINARY PART OF THE NORMALIZED LOAD ADMITTANCE AS CALCULATED FROM EQUATION X-7

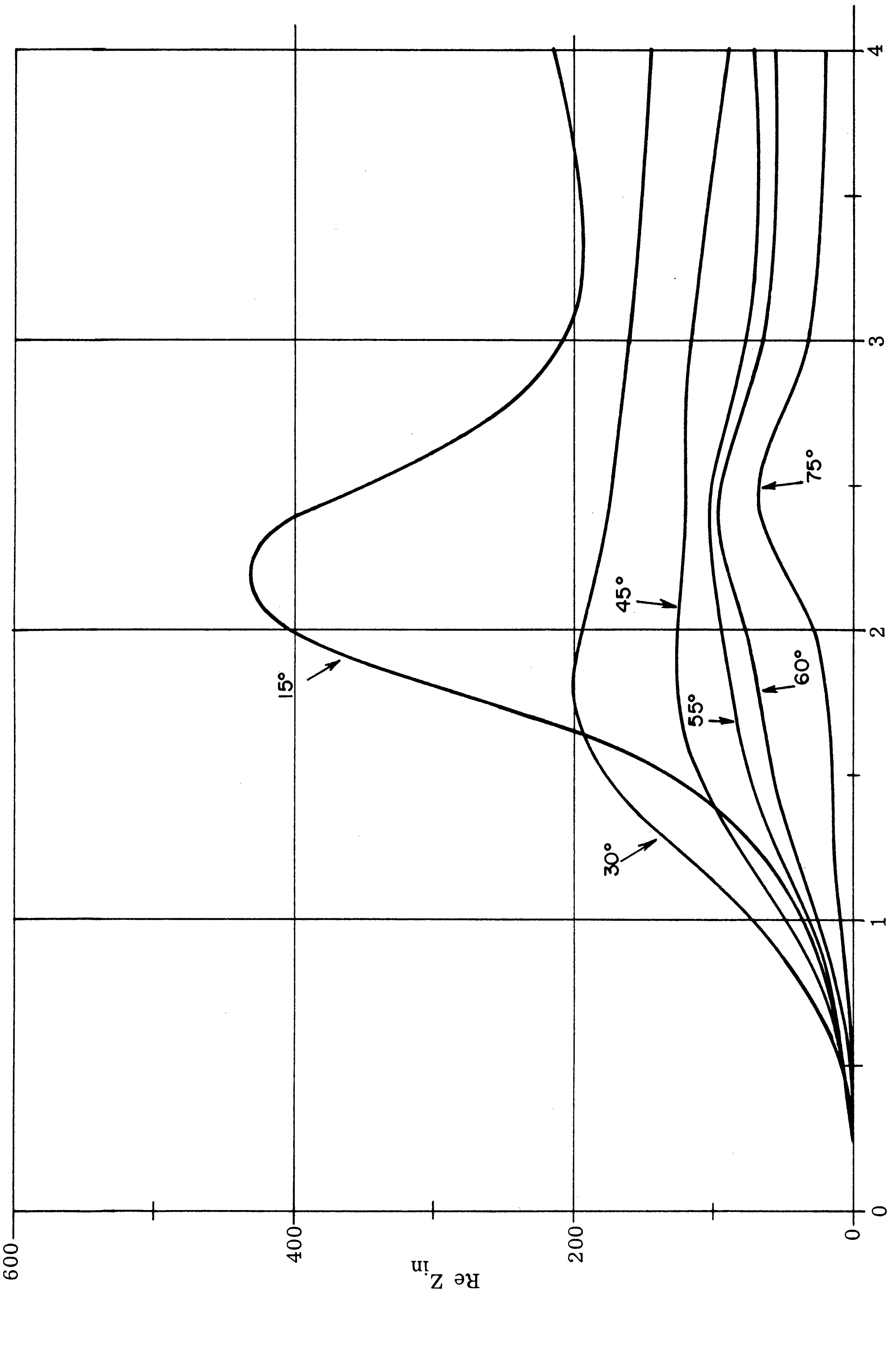

FIGURE 10. THE REAL PART OF THE INPUT IMPEDANCE
AS CALCULATED FROM EQUATION X-7

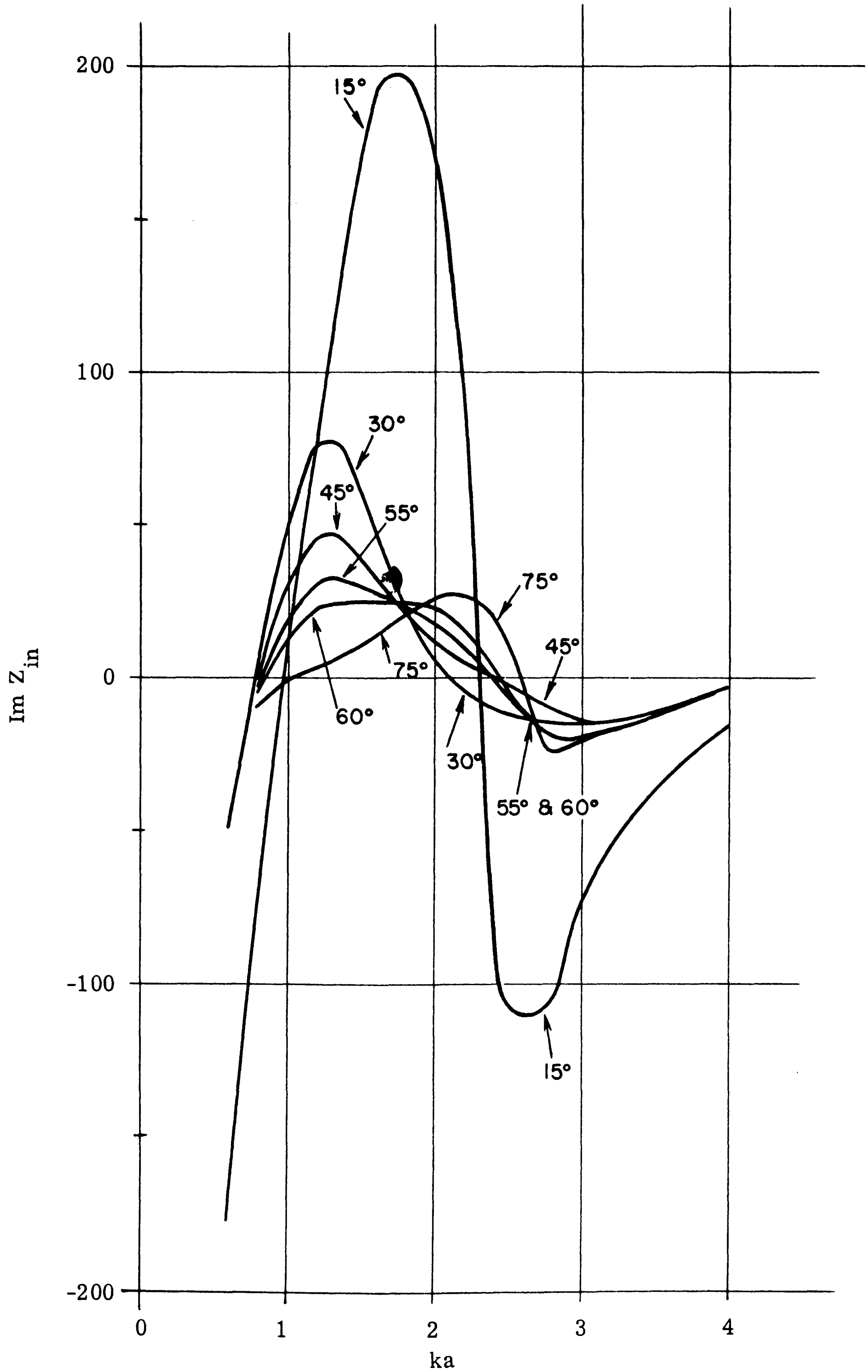

FIGURE 11. THE IMAGINARY PART OF THE INPUT IMPEDANCE AS CALCULATED FROM EQUATION X-7

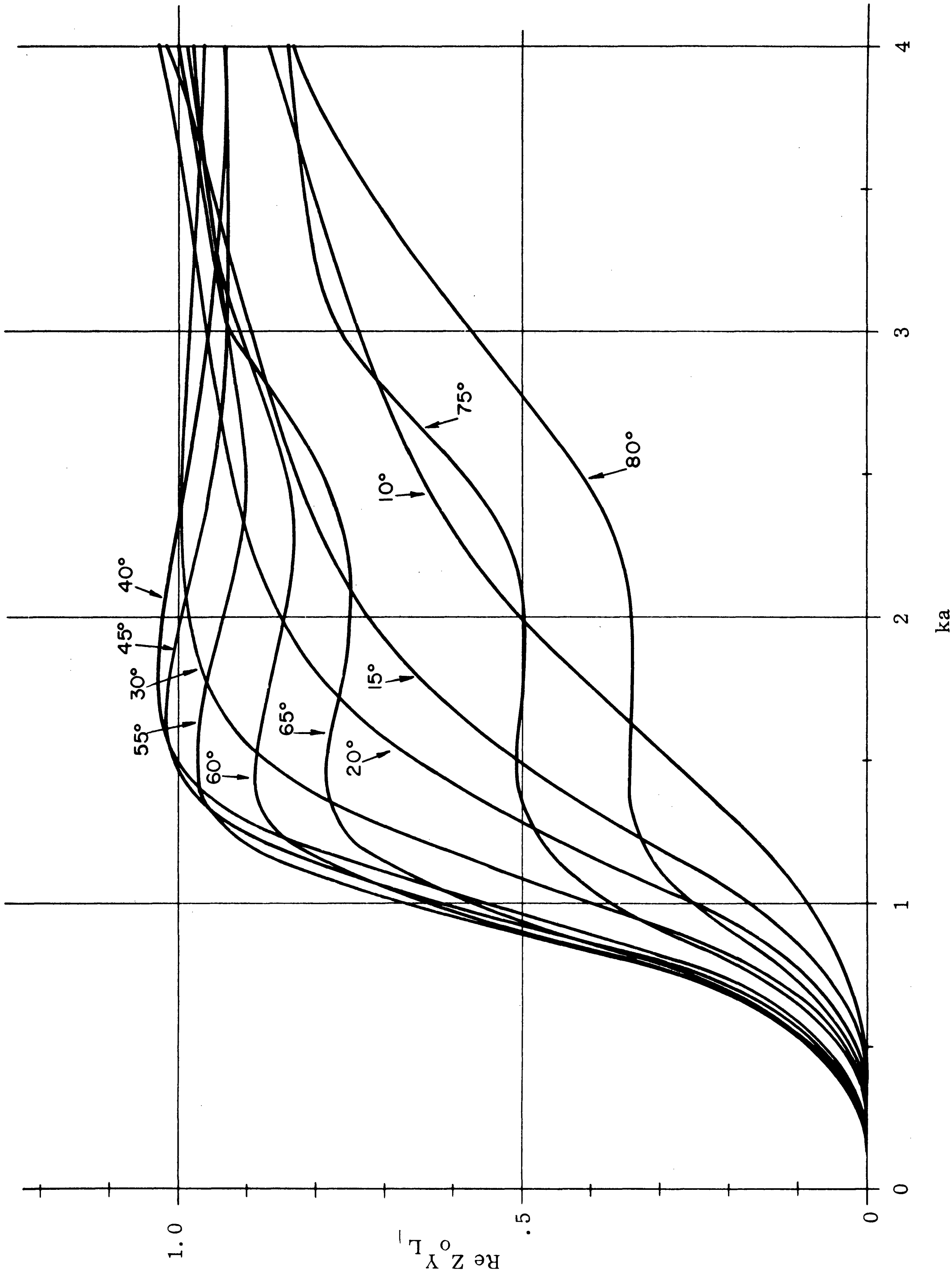

FIGURE 12. THE REAL PART OF THE NORMALIZED LOAD ADMITTANCE AS CALCULATED FROM EQUATION **X**-8

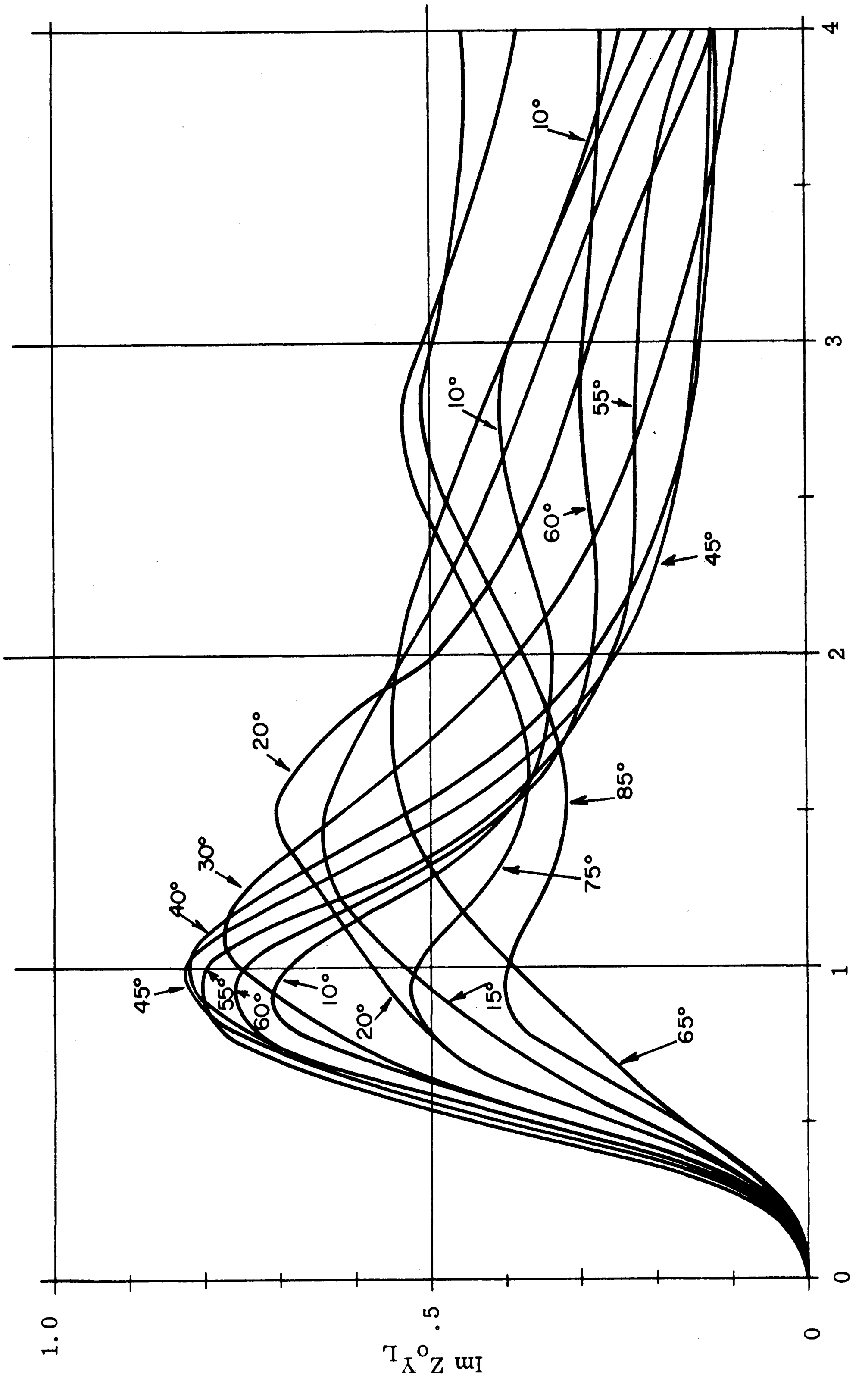

FIGURE 13. THE IMAGINARY PART OF THE NORMALIZED LOAD ADMITTANCE AS CALCULATED FROM EQUATION X-8

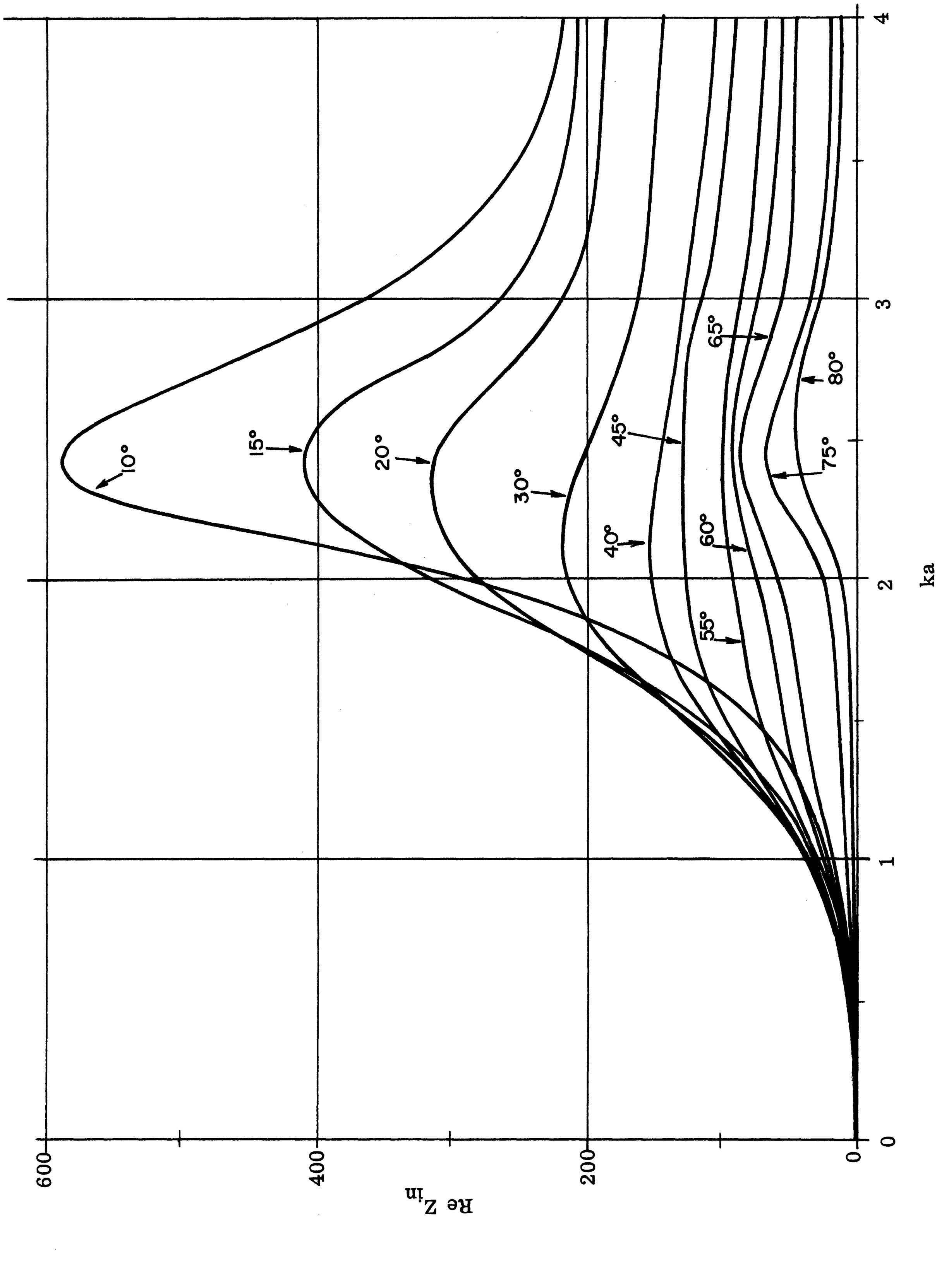

FIGURE 14. THE REAL PART OF THE INPUT IMPEDANCE AS CALCULATED FROM EQUATION X-8

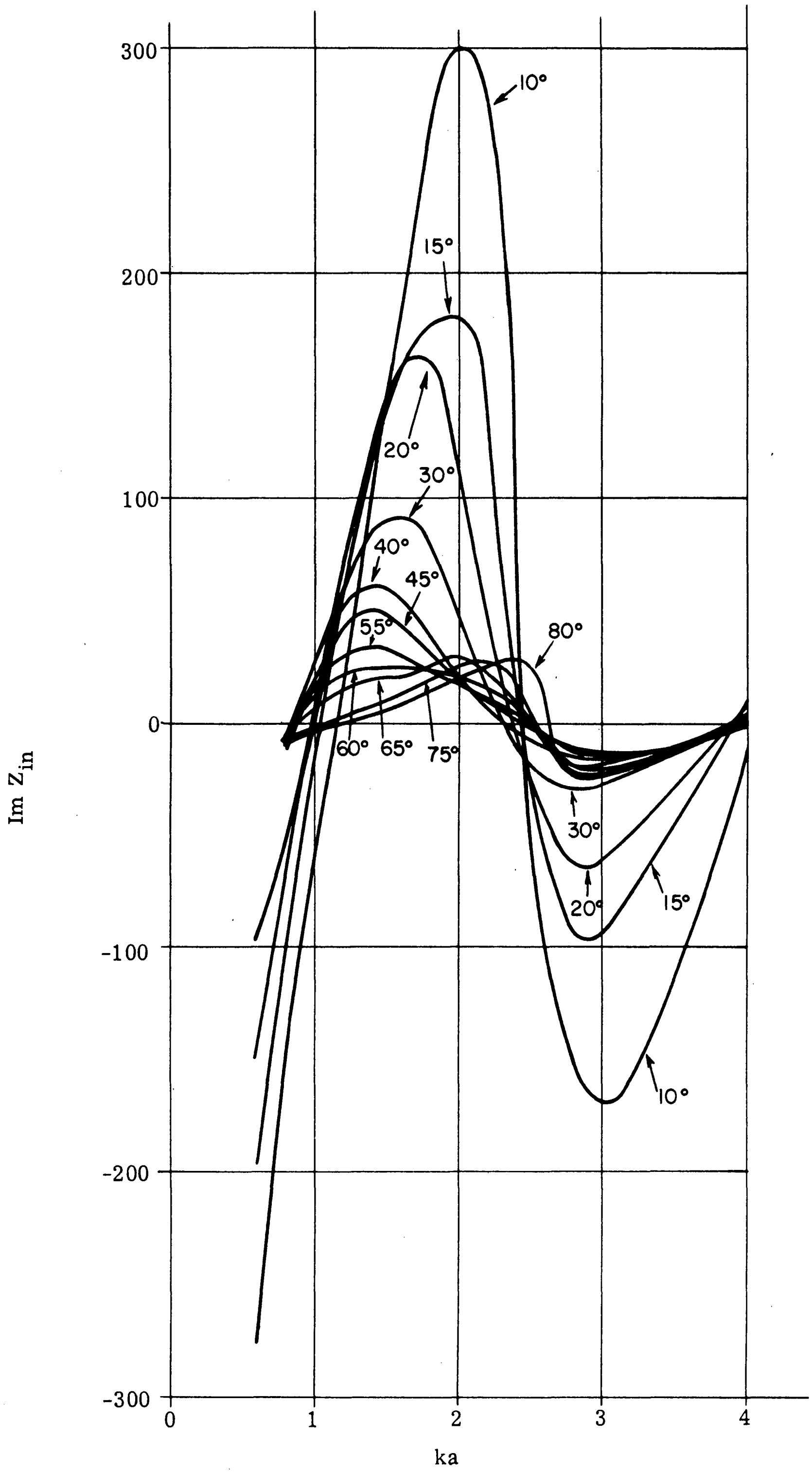

FIGURE 15. THE IMAGINARY PART OF THE INPUT IMPEDANCE AS CALCULATED FROM EQUATION X-8

The results obtained from equation (X-7) and (X-8) agree well for thin and thick cones. However, the agreement is not as good for cones in the 30^{o} range. For these cone angles the method determines b_3 and b_5 very accurately but b_1, which is the dominant term in the expression for load admittance is not as accurately represented. This is illustrated in the subset approximation of equation (X-3) and the graph of Figure 7. For 30^{o} cones a_{n_1} is best approximated by b_3 and a_{n_2} by b_5, thus initially omitting b_1. The final calculation of equation (X-7) will therefore yield a value for b_1, which is too high. Equation (X-8) in general tends to over correct this, so that the final value for b_1 is too low. The primary dependence of the load admittance on b_1, especially for 30^{o} cones*, causes the difference in results.

For thin cones, for example in the case of 15^{o}, b_1 is included in the subset approximation. Thus equations (X-7) and (X-8) agree well. For thick cones of angles greater than 45^{o} higher order corrections are not necessary and again there is good agreement between the two expressions. If more accurate results are desired for cones in the 30^{o} range, a better approximation for the subset must be made. Equation (X-11) utilizes two b's for the initial approximation, expressing a_{n_1} by b_1 and b_3. A sample calculation for a 30^{o} biconical antenna (ka = 1) using equation (X-11) was carried out on the IBM-704. The results are

---

*Since $P_1(\cos\frac{\pi}{6}) > P_3(\cos\frac{\pi}{6}) > P_5(\cos\frac{\pi}{6})$

$$Z_o\, Y_L = .6169 + i\, .8983$$

$$Z_{in} = 52 + i\, 39$$

which is a more valid, solution for this particular cone. The above value for $Z_o\, Y_L$ differs by 17 percent in magnitude from that obtained by using equation (X-7) and by 21 percent using equation (X-8).

Since equation (X-7) yields under-corrected and equation (X-8) over-corrected results, a quick improvement in the answers can be obtained by averaging these two results and plotting a set of four new graphs. However, this was not done here, since in most cases the difference from the two sets of graphs already plotted would be too little to be detectable on the new set of graphs.

APPENDIX A

The Boundary Condition on the Caps of the Biconical Antenna

It is desired to show pointwise convergence of the E_θ field on the caps. However to do this the exact solution must be known first. The strong convergence

$$\int_0^{\pi} \left| \text{Exterior}\,(\theta, \ell) - \text{Interior}\,(\theta, \ell) \right|^2 \sin\theta \, d\theta$$

can be shown explicitly but it suffices to say that whenever expansions in orthogonal functions are made convergence in the mean is implied. To show that the field on the caps goes to zero we start by stating convergence in the mean

$$\int_{\text{all space}} \left| E - I \right|^2 d\Omega = 0$$

Now

$$\int_{\text{all space}} \left| E - I \right|^2 d\Omega = \int_{\text{caps}} \left| E - I \right|^2 d\Omega + \int_{\text{aperture}} \left| E - I \right|^2 d\Omega$$

Since the quantities involved are all positive

$$\int_{\text{all space}} \left| E - I \right|^2 d\Omega \geq \int_{\text{caps}} \left| E - I \right|^2 d\Omega$$

$$\therefore \int_{\text{caps}} \left| E - I \right|^2 d\Omega = 0$$

and since $I_{cap} = 0$

$$\int_{cap} |E|^2 \, d\Omega = 0 \text{ or any subregion of the cap}$$

Therefore

$$\left| E_{cap} \right|^2 = 0 \text{ almost everywhere.}$$

A. A Derivation of the Infinite Matrix for b_m [3, 6].

A derivation of the infinite matrix for b_m which shows that the condition

$$\text{Exterior}_\theta \; (r = \ell, \; \theta) = 0 \text{ for } \theta < \theta_o \tag{1}$$

is included in the derivation of the infinite matrix for b_m follows. The interior (I) and exterior (II) magnetic fields are

$$\ell H_\phi^{I} = \frac{Y_L \; V(\ell)}{2\pi \sin\theta} + \frac{1}{2\pi} \sum_n^{\infty} \frac{a_n}{n(n+1)} \frac{d}{d\theta} L_n(\cos\theta) \quad \theta_o < \theta < \pi - \theta_o \tag{2}$$

$$\ell H_\phi^{II} = \frac{1}{2\pi} \sum_{k=1,3}^{\infty} \frac{b_k}{k(k+1)} \frac{d}{d\theta} P_k(\cos\theta) \quad 0 \geqslant \theta \leqslant \pi \tag{3}$$

In the aperture the outside and inside fields must match, thus

$$H_\phi^{I} \; (r = \ell) = H_\phi^{II} (r = \ell) \quad \theta_o < \theta < \pi - \theta_o \tag{4}$$

Substitute the field expressions in this last equation (4), multiply both sides by

$\sin\theta \dfrac{d}{d\theta} L_s(\cos\theta)$ and integrate both sides between $\theta = \pi - \theta_o$ and $\theta = \theta_o$ to obtain

$$a_s = \frac{2s+1}{\dfrac{\partial L_s(\cos\theta_o)}{\partial s}} \sum_{m=1,3}^{\infty} \frac{b_m P_m(\cos\theta_o)}{m(m+1) - s(s+1)} \tag{5}$$

The electric fields in both regions are

$$\ell E_\theta^{II} = \frac{i\eta}{2\pi} \sum_{k=1,3}^{\infty} \frac{b_k}{k(k+1)} \frac{R_k'}{R_k} \frac{d}{d\theta} P_k(\cos\theta) \qquad 0 \leqslant \theta \leqslant \pi \tag{6}$$

$$\ell E_\theta^{I} \begin{cases} = \dfrac{\eta V(\ell)}{2\pi z_o \sin\theta} - \dfrac{i\eta}{2\pi} \displaystyle\sum_{n}^{\infty} \frac{a_n}{n(n+1)} \frac{S_n'}{S_n} \frac{d}{d\theta} L_n(\cos\theta) & \theta_o < \theta < \pi - \theta_o \\ = 0 & 0 < \theta < \theta_o \text{ and } \pi - \theta_o < \theta < \pi \end{cases} \tag{7}$$

again at the aperture and caps now

$$E_\theta^{II}(r = \ell) = E_\theta^{I}(r = \ell) \qquad 0 \leqslant \theta \leqslant \pi \tag{8}$$

Over the ends of the dipoles, the E_θ field is tangetial to the metallic surface, and therefore vanishes. The functions $dP_k/d\theta$ have certain orthogonal properties that allow the coefficients b_k to be fixed in such a way that the tangential field vanishes over the ends of the cones, and the fields match over the boundary sphere between the cones. The coefficients b_k here play the same sort of part as the coefficients in a Fourier's series, and the external field is being made to fit an arbitrary function at the boundary sphere. The arbitrary function is one which is zero over the ranges of $\theta = 0$ to θ_o, and $\pi - \theta_o$ to π, and is equal to the inside field between the cones.

Thus first expressing b_k in terms of ℓE_θ^{II} by multiplying ℓE_θ^{II} by $\sin\theta \frac{d}{d\theta} P_r(\cos\theta)$ and integrating between 0 and π we get

$$b_k^{\bullet} = \frac{R_k}{R'_k} \pi (2k+1) \int_0^\pi (\ell E_\theta^{II}) \sin\theta \frac{d}{d\theta} P_k (\cos\theta)\, d\theta \tag{9}$$

Using the condition (8) that the field must match across the aperture and the caps we have

$$b_k = \pi(2k+1) \frac{R_k}{R'_k} \int_0^\pi (\ell E_\theta^{I}) \sin\theta \frac{d}{d\theta} P_k (\cos\theta)\, d\theta \tag{10}$$

Substituting equation (7) for ℓE_θ^I and integrating the resulting equation between $\theta = \theta_o$ and $\theta = \pi - \theta_o$ will give

$$b_k = - i P_k (2k+1) \frac{R_k}{R'_k} \left[1 + i r (r+1) \sum_n \frac{a_n}{n(n+1)} \frac{\sin\theta_o}{n(n+1)} \frac{S'_n}{S_n} \frac{\partial L_n}{\partial\theta} \right] \tag{11}$$

The fact that the tangential field on the caps vanishes accounts for the fact that the limits of integration appear as $\theta = \theta_o$ and $\theta = \pi - \theta_o$ instead of $\theta = 0$ and $\theta = \pi$. When equation (5) for a_n is substituted in this last expression for b_k the infinite matrix (equation II-10) for b_k results. This set of equations, therefore, fixes the coefficients b_k in such a way that the field vanishes over the ends of the dipoles, and the outside field matches the inside E_θ field over the boundary surface. Introducing the values of a_n from the set of equations (5) introduces the conditions that the E_r and H_ϕ fields shall also match on the boundary surface. Therefore, if the set of numbers b_k is determined from the infinite matrix, the boundary conditions will be satisfied if an infinite number of terms are used.

B. The Cap Boundary Condition for Very Thick Cones

To show the vanishing of the tangential electric field for arbitrary cones without knowing the exact solution for the mode coefficients b would be difficult. However, it can be shown explicitly that the E_θ field vanishes on the caps for infinitesimally thick cones, i.e. when $\theta_o \longrightarrow \frac{\pi}{2} - \epsilon$. The exterior tangential field on the caps is given by

$$E_\theta(\theta, \ell) = \frac{\eta}{i2\pi\ell} \sum_m^{\infty} \frac{b_m}{m(m+1)} \frac{R'_m(k\ell)}{R_m(k\ell)} \frac{d}{d\theta} P_m(\cos\theta)$$

The coefficients b_m for infintesimally thick cones are derived in Section IX-C. For θ_o near $\frac{\pi}{2}$ they are given by

$$\lim_{\theta_o \to \frac{\pi}{2} - \epsilon} b_m = - i\,(2m + 1)\, P_m(\sin \epsilon) \frac{R_m(k\ell)}{R'_m(k\ell)}$$

Substituting these in the above expansion the tangential field on the caps of infinitesimally thick cones will be given thus

$$\lim_{\theta_o \to \frac{\pi}{2} - \epsilon} E_\theta(\theta, \ell) = \frac{-\eta}{2\pi\ell} \sum_m^\infty \frac{2m+1}{m(m+1)} P_m(\sin\epsilon) \frac{d}{d\theta} P_m(\cos\theta)$$

Now this expression looks like the expansion of a delta function in Legendre polynomials. Thus a derivation of the delta function will be given first. Let

$$\delta(\theta_o, \theta) = \sum_m^\infty c_m \frac{d}{d\theta} P_m(\cos\theta)$$

multiplying by $\frac{d}{d\theta} P_r(\cos\theta)\sin\theta$ and integrating will determine the coefficients c_m

$$\int_0^\pi \delta(\theta_o, \theta) \frac{d}{d\theta} P_r(\cos\theta)\sin\theta\, d\theta = \sum_m^\infty c_m \int_0^\pi \frac{d}{d\theta} P_m(\cos\theta) \cdot$$

$$\cdot \frac{d}{d\theta} P_r(\cos\theta)\sin\theta\, d\theta = c_r \frac{2r(r+1)}{2r+1}$$

Substituting this result in the above expansion

$$\delta(\theta_o, \theta) = \frac{1}{2} \sum_m^{\infty} \frac{2m+1}{m(m+1)} \int_0^{\pi} \delta(\theta_o, \theta') \frac{d}{d\theta'} P_m(\cos\theta') \sin\theta' \, d\theta' \cdot \frac{d}{d\theta} P_m(\cos\theta)$$

Performing the indicated integration will give the desired expansion for the delta function

$$\delta(\theta_o, \theta) = \frac{1}{2} \sum_m^{\infty} \frac{2m+1}{m(m+1)} \frac{d}{d\theta_o} P_m(\cos\theta_o) \frac{d}{d\theta} P_m(\cos\theta)$$

The expression for $\lim_{\theta_o \to \frac{\pi}{2} - \epsilon} E_\theta(\theta, \ell)$ looks similar to the expression for $\delta(\theta_o, \theta)$ except that $\frac{d}{d\theta} P_m(\cos\theta_o)$ occurs in the delta function expression and $P_m(\cos\theta_o)$ in the expression for the field E_θ. However in the limit as $\theta_o \to \frac{\pi}{2} - \epsilon$ a relation between these two exist which is

$$P_m(\sin\epsilon) = -\epsilon \frac{dP_m(\sin\epsilon)}{d\epsilon} \qquad \text{for } m = 1, 3, 5, \ldots$$

Substituting this into the expression for E_θ

$$\lim_{\theta_o \to \frac{\pi}{2} - \epsilon} E_\theta(\theta, \ell) = \frac{\eta}{2\pi \ell} \epsilon \sum_m^{\infty} \frac{2m+1}{m(m+1)} \frac{dP_m(\sin\epsilon)}{d\epsilon} \frac{d}{d\theta} P_m(\cos\theta)$$

Comparing this to the delta function expression, the E_θ field can be stated as follows

$$\lim_{\theta_o \to \frac{\pi}{2} - \epsilon} E_\theta (\theta, \ell) = - \frac{\eta}{\pi \ell} \epsilon \; \delta(\frac{\pi}{2} - \epsilon, \; \theta)$$

Thus E_θ vanishes every place on the caps, except for the circumferential ring source which is expressed by the delta function.

APPENDIX B

Explanation of Abbreviated Symbols

$$R_r = R_r(k\ell) = (k\ell)^{1/2}\, H^{(2)}_{r+1/2}(k\ell) \qquad \text{(II-8)}$$

$$S'_{n_i} = \frac{d}{dk\ell}\, S_{n_i}(k\ell) = \frac{d}{dk\ell}\,(k\ell)^{1/2}\, J_{n_i+\frac{1}{2}}(k\ell) \qquad \text{(II-9)}$$

$$P_r = P_r(\cos\theta_o) \qquad P_r \sim \frac{1}{\sqrt{r}}, \quad r \to \infty$$

$$P'_r = \frac{d}{d\theta_o}\, P_r(\cos\theta_o) \qquad P'_r \sim \sqrt{r}, \quad r \to \infty$$

$$\frac{\partial L_{n_i}}{\partial\theta_o} \Big/ \frac{\partial L_{n_i}}{\partial n_i} = -\frac{dn_i}{d\theta_o}$$

$$L_{n_i} = \frac{1}{2}\left(P_{n_i}(\cos\theta) - P_{n_i}(-\cos\theta)\right) \qquad \text{(II-3)}$$

$$n_i^o = \frac{2\pi}{\pi - 2\theta_o}\, i - \frac{1}{2} = \rho\, i - \frac{1}{2} \qquad \text{(III-2, VI-3)}$$

$$n_i = n_i^o - \frac{\cot\theta_o}{8\pi\, i + 4(\pi - 2\theta_o)} \qquad \text{(III-11)}$$

$$B_r = -\,i(2r+1)\, P_r \frac{R_r}{R'_r} \qquad \text{(VII-2)}$$

N_r^m = is given by equation (VI-2)

$$I_r^m = \frac{1}{\alpha_r} P_m N_r^m \tag{VII-4}$$

$$J_r N_r' - J_r' N_r = \frac{2}{\pi k\ell}, \quad J_r H_r' - J_r' H_r = \frac{-2i}{\pi k\ell}$$

$$S_r R_r' - R_r S_r' = -\frac{2i}{\pi} \tag{VII-17}$$

$$\frac{d}{dk\ell} H_r(k\ell) = \frac{r}{k\ell} H_r(k\ell) - H_{r+1}(k\ell)$$

$$\frac{J_n'(k\ell)}{J_n(k\ell)} = \frac{n}{k\ell} - \frac{J_{n+1}(k\ell)}{J_n(k\ell)}$$

$$\frac{S'}{S} = \frac{S_{n_i}'(k\ell)}{S_{n_i}(k\ell)} = \frac{n_i+1}{k\ell} - \frac{J_{n_i+3/2}(k\ell)}{J_{n_i+1/2}(k\ell)}$$

$$\frac{J_{n+1}(k\ell)}{J_n(k\ell)} \sim \frac{k\ell}{2} \frac{1}{n+1}, \qquad n \to \infty$$

$$\frac{H_{n+1}(k\ell)}{H_n(k\ell)} \sim \frac{n}{k\ell}, \qquad n \to \infty$$

$$\frac{S_n'(k\ell)}{S_n(k\ell)} \sim \frac{n}{k\ell}, \qquad n \to \infty$$

$$\frac{R_n'(k\ell)}{R_n(k\ell)} \sim \frac{n}{k\ell}, \qquad n \to \infty$$

APPENDIX C

Electromagnetic Radiation From a Cylindrically Capped Bi-Wedge

This appendix is completely self contained. Before a study of the biconical antenna was started it was felt desirable to solve a simpler radiation problem. The bi-wedge is such a problem since it is the two-dimensional counterpart of the biconical antenna.

ABSTRACT

The cylindrically capped bi-wedge is an arrangement of two perfectly conducting wedges, apex to apex and exactly opposing; it is truncated by a cylinder whose axis is the apex of the bi-wedge. A line source at the apex excites this geometry. To find what the radiation properties of this configuration of conductors are the corresponding boundary value problem is solved.

Truncating the bi-wedge by a cylinder defines two regions — the interior and the exterior. The fields in the interior and exterior region are given by appropriate series expansions which are solutions to Maxwell's equations. A relationship between the coefficients of the two fields is obtained when the fields are matched across the aperture. A set of infinite simultaneous equations is generated. These can be solved for the coefficients to which special summation techniques have been applied to make a truncation of the infinite matrix valid. The radiated field of a bi-wedge is then expressed as a series with unknown coefficients. These can now be calculated by solving a set of finite simultaneous

equations. A bi-wedge in the resonance region was chosen to illustrate this procedure. The computations for ka = $\frac{\pi}{2}$ were performed and the far-field radiation patterns plotted for various wedge angles. The limiting cases of the Rayleigh region, the thin bi-wedge, and the bi-wedge when the angle θ_o approaches $\frac{\pi}{2}$ are then analyzed. It is found that for the thin and the very thick bi-wedge the matrix decouples and the field can be given exactly for these two limiting cases.

INTRODUCTION

The cylindrically capped bi-wedge is an arrangement of two infinite wedges, apex to apex and exactly opposing. The wedge is truncated by a cylinder. Figure 1 shows the geometry; for clarity only a semi-infinite bi-wedge is shown.

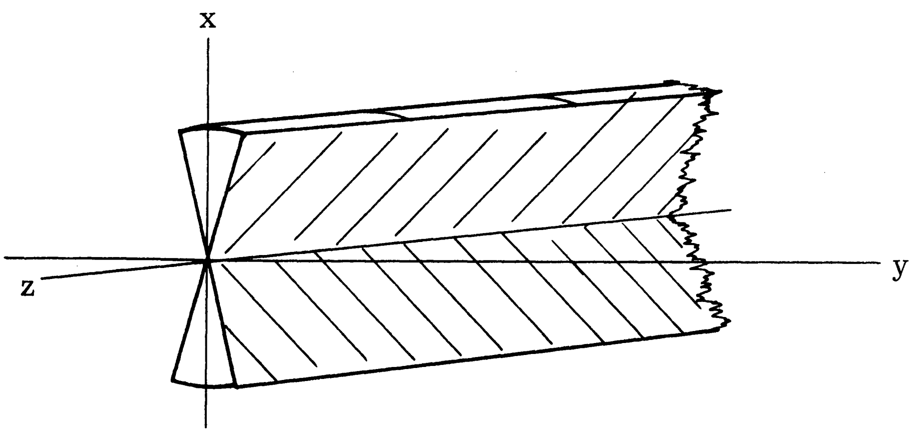

FIGURE 1. THE SEMI-INFINITE BI-WEDGE

The problem is formulated in cylindrical coordinates. Figure 2 shows a cross section and some notation of the bi-wedge. If the bi-wedge is considered

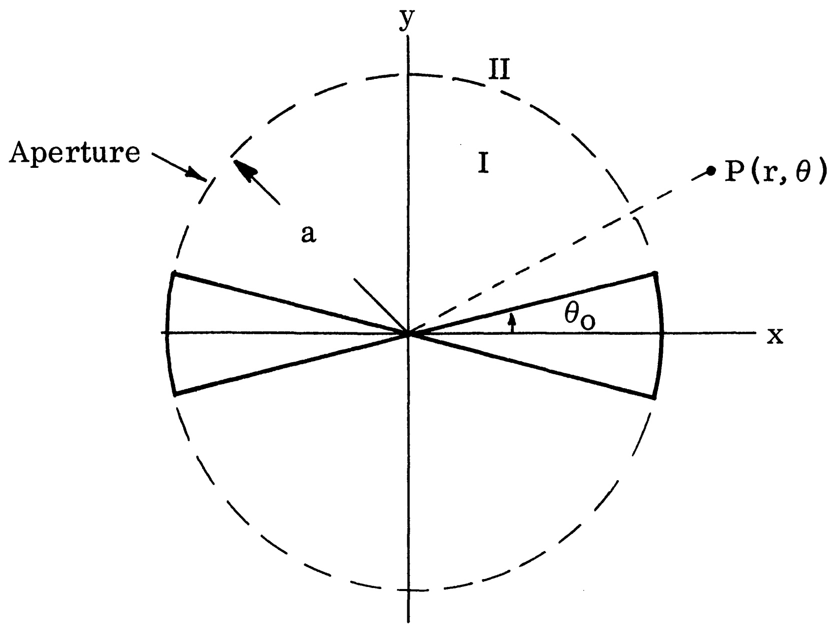

FIGURE 2. CROSS SECTION AND NOTATION OF BI-WEDGE, WHERE I CORRESPONDS TO THE INTERIOR REGION, II CORRESPONDS TO THE EXTERIOR REGION

as a radiator, it can be conveniently excited at the apices by a line source of the magnetic or electric type. The magnetic line source could be a solenoid of infinite length and infinitesimally small loop diameter carrying a current. This excitation would generate a field with H_z, E_θ, and E_r components and an infinity of modes, which are the TM modes. The electric line source can be a conducting wire carrying a current, which would give rise to a field with E_z, H_θ, H_r components only, and an infinity of TE modes. These two solutions are entirely symmetric; i.e., if the fields due to a magnetic line source are known, the fields for an electric line source can be obtained by an interchange of subscripts on corresponding field components.

The electromagnetic fields in the interior and exterior region are then given by appropriate series expansions with arbitrary coefficients, which are solutions to Maxwell's equations. A relationship between the coefficients of the two fields is obtained when the fields are matched across the aperature.

THE ELECTROMAGNETIC FIELD OF A BI-WEDGE

I. The Interior Field

A general wedge-type solution to Maxwell's equations for the interior region is

$$H_z = \sum_{\nu} \left(A_\nu J_\nu(kr) + B_\nu N_\nu(kr)\right) \left(C_\nu \cos\nu\theta + D_\nu \sin\nu\theta\right)$$

For the field to be finite at the origin $B_\nu \equiv 0$. Applying boundary conditions at the surface of the wedge

$$E_r(\theta_o) = 0 \qquad\qquad r \leqslant a$$

$$E_r(\pi - \theta_o) = 0$$

will yield two homogeneous simultaneous equations for the coefficients C_ν and D_ν. For this set to have any nontrivial solutions the deterimant must be zero. This gives a trigonometric relationship for the separation constant ν, which when solved is

$$\nu = \frac{\pi}{\pi - 2\theta_o} i \qquad\qquad i = 0, 1, 2, \ldots$$

One of these homogeneous equations can be used to express C_ν in terms of D_ν, then introducing a new constant the interior magnetic field can be stated as

$$H_z^I = \sum_{\nu = 0}^{\infty} a_\nu \frac{J_\nu(kr)}{J_\nu(ka)} \cos\nu\,(\theta - \theta_o).$$

If the radiation characteristics of the bi-wedge are to be determined it can conveniently be excited locally by a line source positioned at the apices of the wedges. A magnetic line source which generates a magnetic field in the z-direction will be used. If the input voltage of the line source is to be finite, i.e.

$$V_{in} = \lim_{r \to 0} \int_{\theta_o}^{\pi - \theta_o} E_\theta \, r\, d\theta$$

then E_θ in the neighborhood of the origin must have a $\frac{1}{r}$ type behaviour. Therefore, if the Neumann function is chosen to represent the magnetic line source, E_θ in the above expression can be given by

$$E_\theta \sim N_1(kr)$$

Furthermore the coaxial magnetic field H_z of the line source will excite surface currents given by

$$\underline{J} = \underline{n} \times \underline{H}$$

which flow in the same direction on the wedge planes of each aperture. Surface currents which flow in the same direction are given by the even modes thus

$$\nu = \frac{\pi}{\pi - 2\theta_o} i = n_i \qquad i = 0, 2, 4, \ldots$$

The even modes also correspond to the vanishing of the tangential electric field along the symmetry plane $\theta = \pm \frac{\pi}{2}$, i.e.

$$E_r(\theta) = - E_r(\pi - \theta)$$

This is a convenient condition, since a perfectly conducting thin plane can be placed there without disturbing the electromagnetic field. This permits the use of image analyses to obtain immediately the field of a single capped wedge above ground.

The complete interior field including the source can now be expressed as

$$H_z^I(r,\theta) = \sum_{i=2,4}^{\infty} a_{n_i} \frac{J_{n_i}(kr)}{J_{n_i}(ka)} \cos n_i \left(\theta - \frac{\pi}{2}\right) + a_o \frac{J_o(kr)}{J_o(ka)} + c_o \frac{N_o(kr)}{N_o(ka)}$$

$$E_\theta^I(r,\theta) = -\frac{1}{j\omega\epsilon} \sum_{i=2,4}^{\infty} a_{n_i} \frac{\partial}{\partial r} \frac{J_{n_i}(kr)}{J_{n_i}(ka)} \cos n_i \left(\theta - \frac{\pi}{2}\right) +$$

$$+ \frac{i}{j}\sqrt{\frac{\mu}{\epsilon}} \left(a_o \frac{J_1(kr)}{J_o(ka)} + c_o \frac{N_1(kr)}{N_o(ka)}\right)$$

$$E_r^I(r,\theta) = \frac{-1}{j\omega\epsilon r} \sum_{i=2,4}^{\infty} n_i a_{n_i} \frac{J_{n_i}(kr)}{J_{n_i}(ka)} \sin n_i \left(\theta - \frac{\pi}{2}\right)$$

where the constant c_o is related to the input voltage as follows

$$V_{in} = \frac{j\,2\,c_o(\pi - 2\theta_o)}{\pi k N_o(ka)} \sqrt{\frac{\mu}{\epsilon}}$$

II. The Exterior Field

The exterior region II has a general solution of the following form

$$H_z^{II} = \sum_\nu \left(A_\nu H_\nu^{(1)}(kr) + B_\nu H_\nu^{(2)}(kr)\right)\left(C_\nu \cos\nu\theta + D_\nu \sin\nu\theta\right)$$

To satisfy the radiation condition $A_\nu \equiv 0$. Since the free space fields must be rotationally symmetric with a period of 2π, the free space eigenvalues must be integers. The vanishing of the tangential field on the symmetry plane $\theta = \pm \frac{\pi}{2}$ will again be satisfied for the even integers only. Thus, in the exterior region the complete field is specified by the following equations

$$H_z^{II}(r,\theta) = \sum_{m=0,2,4}^{\infty} b_m \frac{H_m^{(2)}(kr)}{H_m^{(2)}(ka)} \cos m\theta$$

$$E_\theta^{II}(r,\theta) = -\frac{1}{j\omega\epsilon} \sum_{m=0,2,4}^{\infty} b_m \frac{\partial}{\partial r} \frac{H_m^{(2)}(kr)}{H_m^{(2)}(ka)} \cos m\theta$$

$$E_r^{II}(r,\theta) = \frac{-1}{j\omega\epsilon r} \sum_{m=0,2,4}^{\infty} m\, b_m \frac{H_m^{(2)}(kr)}{H_m^{(2)}(ka)} \sin m\theta \;.$$

III. Matching of Fields

A relationship between the interior and exterior mode coefficients a_{n_i} and b_m will be determined when the tangential electric and magnetic fields are matched along the ficticious mathematical boundary circle which separates region I from region II. The magnetic field must then satisfy

$$H_z^{I}(a,\theta) = H_z^{II}(a,\theta) \qquad \theta_o \leqslant \theta \leqslant \pi - \theta_o$$

Substituting the appropriate expression for the interior and exterior fields in the above equation, multiplying by cos $s_i\,(\theta - \frac{\pi}{2})$ and integrating over the orthogonal range of this function which is between θ_o and $\pi - \theta_o$ will yield an expression for an interior mode coefficient

$$a_{s_i} = \frac{-1}{\pi - 2\theta_o} \sum_{m=2,4}^{\infty} b_m \,(-1)^{i/2} \,\frac{m \sin m\theta_o}{m^2 - s_i^2}$$

$$a_o = b_o - c_o - \frac{2}{\pi - 2\,\theta_o} \sum_{m=2,4}^{\infty} b_m \,\frac{\sin m\,\theta_o}{m} \quad .$$

Now the tangential electric field along the ficticious boundary and the caps is matched, i.e.

$$E_\theta^{I}\,(a, \theta) = E_\theta^{II}\,(a, \theta) \qquad\qquad 0 \leqslant \theta \leqslant \pi$$

Substituting the field expressions into the above relationship, multiplying by cos $r\,\theta$, integrating between 0 and π, but reducing the limits of integration for the interior field to θ_o and $\pi - \theta_o$ to account for the vanishing of the electric field inside the perfectly conducting wedge and in doing so also satisfying the boundary condition on the caps which is

$$E_\theta^{II}\,(a, \theta) = 0, \qquad\qquad 0 \leqslant \theta \leqslant \theta_o$$

an expression for the exterior mode coefficients results which is

$$b_r = -\frac{4}{\pi}\frac{H_r}{H_r'}\sum_{i=2,4}^{\infty} a_{n_i}\frac{J_{n_i}'}{J_{n_i}}\frac{(-1)^{i/2}\, r\sin r\theta_o}{r^2 - n_i^2} -$$

$$-\frac{4}{\pi}\frac{H_r}{H_r'}\frac{\sin r\theta_o}{r}\left(a_o\frac{J_o'}{J_o} + c_o\frac{N_o'}{N_o}\right)$$

$$b_o = \frac{\pi - 2\theta_o}{\pi}\frac{H_o}{H_o'}\left(a_o\frac{J_o'}{J_o} + c_o\frac{N_o'}{N_o}\right) .$$

In the above expression the unspecified arguments of all Bessel functions are ka, Hankel functions are of the second kind and the primes signify a differentiation with respect to the argument.

An infinite set of simultaneous equations for the interior mode coefficients or the exterior mode coefficients can now be obtained from these expressions. Since the electromagnetic field exterior to the structure is of more interest, an infinite matrix for the coefficients b_m will be derived by substituting the expression for a single interior mode into that for a single exterior mode. The result is the set of equations

$$\frac{4}{\pi - 2\theta_o} \sum_{m=2,4}^{\infty} b_m\, r\, m \sin r\theta_o \sin m\theta_o \left(2 \sum_{i=2,4}^{\infty} \frac{J'_{n_i} \big/ J_{n_i}}{(m^2 - n_i^2)(r^2 - n_i^2)} - \right.$$

$$\left. - \frac{\pi}{2 r^2 m^2} \frac{ka\, J_1\, H_1}{j + \theta_o\, ka\, J_1\, H_o} \right) - b_r \frac{\pi}{2} \frac{H'_r}{H_r} =$$

$$= \frac{2 \sin r\,\theta_o}{r\, N_o} \frac{H_1\, c_o}{j + \theta_o\, ka\, J_1\, H_o}$$

and

$$b_o = \frac{- H_o}{j + \theta_o\, ka\, J_1\, H_o} \left(\frac{c_o(\pi - 2\theta_o)}{\pi\, N_o} + ka\, J_1 \sum_{m=2,4}^{\infty} b_m \frac{\sin m\theta_o}{m} \right).$$

A solution of this infinite set for b_m would completely determine the electromagnetic field radiated from a bi-wedge. Graphs of Radiation patterns can be obtained by first substituting the far-field approximation of the Hankel functions in the exterior field expressions and normalizing with respect to the source constant c_o. Thus

$$\lim_{r \to \infty} \frac{H_z^{II}(r,\theta)}{c_o/N_o} = \sqrt{\frac{2}{\pi kr}}\; e^{-i(kr - \frac{\pi}{4})} \sum_{m=0,2,4}^{\infty} \frac{b_m}{c_o/N_o} \frac{(-1)^{\frac{m}{2}}}{H_m} \cos m\theta$$

where

$$g(\theta) = \sum_{m=0,2,4}^{\infty} \frac{b_m}{c_o/N_o} \frac{(-1)^{\frac{m}{2}}}{H_m} \cos m\theta$$

specifies the radiation patterns.

THE RAYLEIGH REGION

In the long-wavelength limit the higher order modes vanish and only the lowest modes need be considered. The magnetic field can be approximated for ka $\ll$ 1 as

$$H_z^{II}(r,\theta) = \frac{\pi b_o H_o^{(2)}(kr)}{\pi - j2 \ln ka} - j\frac{\pi}{4} b_2 (ka)^2 H_2^{(2)}(kr) \cos 2\theta + \mathcal{O}(ka)^4$$

The mode coefficient b_2 must nevertheless be obtained from the infinite matrix. When the asymptotic expressions for ka $<<$ 1 are utilized and higher order terms neglected the infinite matrix reduces to the simpler form of

$$\frac{8}{\pi - 2\theta_o} \sum_{m=2,4}^{\infty} b_m \, r m \sin r\theta_o \sin m\theta_o \sum_{i=2,4}^{\infty} \frac{n_i}{(m^2 - n_i^2)(r^2 - n_i^2)} -$$

$$- b_r r \frac{\pi}{2} = 2 \frac{\sin r\theta_o}{r} \frac{c_o}{\ln ka}$$

$$b_o = \frac{(j\pi + 2\ln ka)(\pi - 2\theta_o)\, c_o}{2\pi \ln ka} .$$

The above matrix is dependent on ka. To make these equations independent of ka one can multiply both sides by ln ka and solve the simultaneous set for

$$b'_m = b_m \ln ka$$

Therefore the radiated magnetic field with correct ka dependence for the Rayleigh region is

$$H_z^{II}(r,\theta) = \frac{j(\pi - 2\theta_o)c_o}{2 \ln ka} H_o^{(2)}(kr) - j\frac{\pi}{4} b_2' \frac{(ka)^2}{\ln ka} H_2^{(2)}(kr) \cos 2\theta + \mathcal{O}(ka)^4$$

THE THIN BI-WEDGE

The thin bi-wedge, i.e., when the angle θ_o tends to zero, resembles a strip excited by a line source at the center. The infinite matrix for b_m decouples in this limiting case and the exterior field can be expressed as an infinite series with known terms. In the limiting case of $\theta_o \rightarrow 0$ all terms in the matrix vanish except those for which

$$m = r = i.$$

Taking this limit and neglecting terms of order θ_o^2 and higher the expression for the exterior mode coefficients is

$$b_r = -2c_o \theta_o ka \frac{H_1 J_r H_r}{N_o}$$

and

$$b_o = jc_o \frac{H_o}{N_o} \left[1 - \theta_o\left(\frac{2}{\pi} - jka J_1 H_o\right)\right].$$

With the above two results the radiation pattern for thin bi-wedges is given by

$$g(\theta) = j \left[1 - \theta_o \left(\frac{2}{\pi} - j ka\, J_1 H_o - j\, 2 ka\, H_1 \sum_{m=2,4}^{\infty} (-1)^{\frac{m}{2}} J_m \cos m\,\theta \right) \right].$$

From the above expressions it can be seen that for infinitesimally thin wedges higher order modes do not exist. The only non-vanishing mode is the dominant mode of the line source. Thus two strips, placed symmetrically opposite each other along the magnetic line source have no effect on the field of the line source. The physical interpretation of this is that the surface currents which are excited by the line source and which in turn generate the higher modes are equal and opposite on the two faces of each wedge, thus cancelling each other as $\theta_o \rightarrow 0$. The boundary condition is automatically satisfied since the field of the line has no radial component.

The following figure displays patterns for thin bi-wedges calculated from the last equation as the length ka is varied. The dashed line is a circle drawn in for reference.

THE BI-WEDGE, WHEN THE ANGLE θ_o APPROACHES 90^o

In the limit when θ_o equals 90^o we have a perfectly conducting, unexcited cylinder. All coefficients should vanish, including that of the dominant mode since

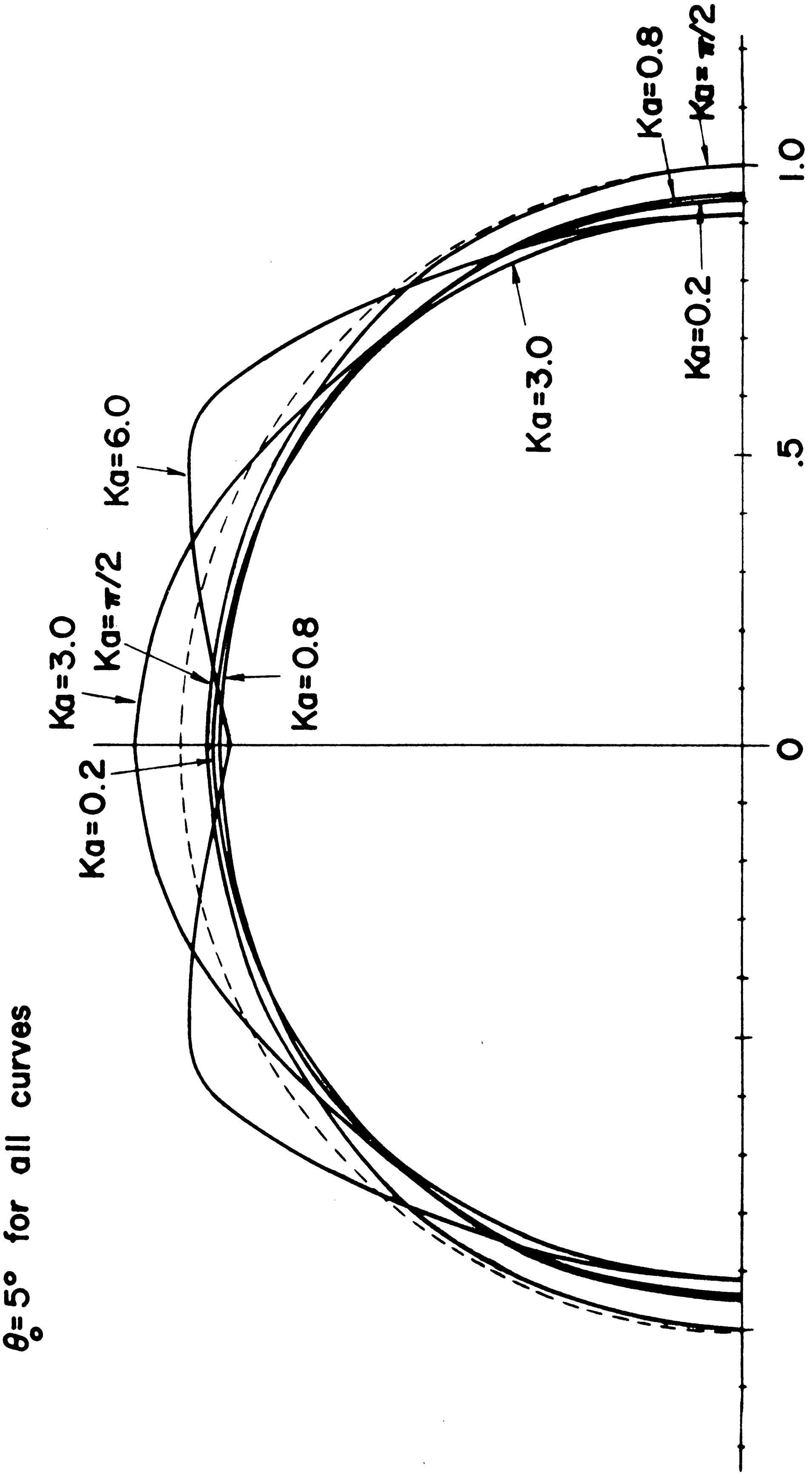

FIGURE 3. RADIATION PATTERNS OF THIN BI-WEDGES

the line source is completely shielded inside the cylinder. However, letting θ_o be almost 90^o, an interesting case of a cylinder excited by two longitudinal slots results. Let

$$\theta_o = \frac{\pi}{2} - \delta .$$

When this is substituted in the infinite matrix and all terms of order δ^2 and higher are neglected the new expression for the higher mode coefficients appropriate for thick bi-wedges is given by

$$b_r = \frac{(-1)^{\frac{r}{2}} 8 H_1 H_r \delta c_o}{\pi N_o H_r' (2j + \pi ka J_1 H_o)}$$

and

$$b_o = \frac{-4 H_o c_o \delta}{\pi N_o (2j + \pi ka J_1 H_o)}$$

The radiation patterns are then determined from

$$g(\theta) = \frac{-4\delta}{\pi(2j + \pi ka J_1 H_o)} \left(1 - 2H_1 \sum_{m=2,4}^{\infty} \frac{\cos m\theta}{H_m'} \right) .$$

Thus as mentioned before the field vanishes as δ approaches zero.

The following figure displays patterns for thick bi-wedges calculated from the above equation as the length ka is varied.

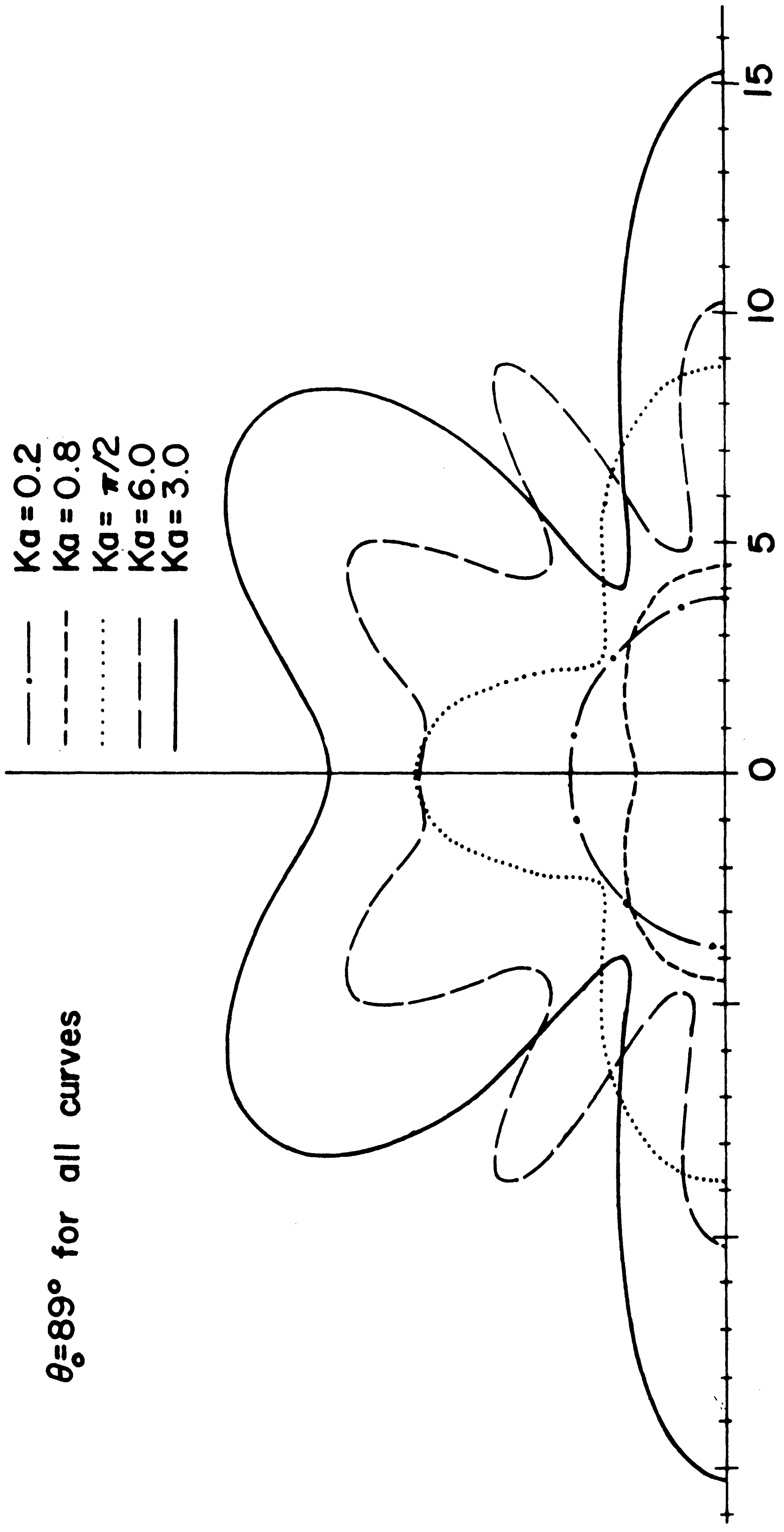

FIGURE 4. RADIATION PATTERNS OF THICK BI-WEDGES

It is interesting to observe that for similar changes in ka the radiation patterns for the thick bi-wedge show much more variation as the corresponding patterns for thin bi-wedges. This is of course due to the shielding of the source by a thick cylinder. For thin bi-wedges b_r vanishes and b_o approaches a constant value, but for thick bi-wedges both b_r and b_o vanish. Since for thick bi-wedges b_r and b_o are of comparable magnitude and when added will yield the rapidly varying patterns.

THE RADIATION PATTERNS FOR BI-WEDGES OF ANY ANGLE

The exterior mode coefficients b_r which are needed in the calculation for the radiation patterns must be obtained from the infinite set of simultaneous equations for bi-wedges of arbitrary angle θ_o. The easiest way to obtain results from an infinite set is to truncate it and solve the finite set. One can hope that the coefficients are rapidly converging, giving good results with low truncation orders, In this analysis before a truncation was performed the summation over the interior modes, i.e. the i-sum in the set of simultaneous infinite equations was transformed into a more rapidly converging series by Kummer's transformation technique. Then, the infinite matrix was truncated to a fourth order matrix and inverted. To check the convergence of the truncation the corresponding second and third order matrices were inverted. A comparison between the results of the third and the fourth order matrix showed little variation. This justified the fourth order matrix as giving results of sufficient accuracy to calculate radiation patterns. The convergence of the coefficients is rapid enough that the exterior field is not significantly altered when higher order coefficients beyond the third (b_6) are included.

The physical interpretation of this truncation is that besides the dominant mode, four exterior modes were included in the matching of the exterior field to the interior field across the aperture. No clear statement on the number of interior modes (given by the number of terms in the i-summation) that were used to approximate the interior field can be made since Kummer's summation technique "mixes up" the interior modes in order to increase the convergence of the i-summation.

The inversion and pattern calculations were performed for bi-wedges in the resonance region ($ka = \frac{\pi}{2}$) and various cone angles. The patterns are shown in Figure 5.

The $\theta_o = 18^o$ graph compares strongly to the corresponding graph in Figure 3 calculated from simple expressions obtained for the limiting case of thin wedges. Similarly, the $\theta_o = 73.6^o$ graph compares strongly to the corresponding graph in Figure 4 calculated from simple expressions for the limiting case of thick wedges. Thus it can be concluded that equations for the coefficients b_r for the two limiting cases are valid far beyond the limiting angles of zero and ninety

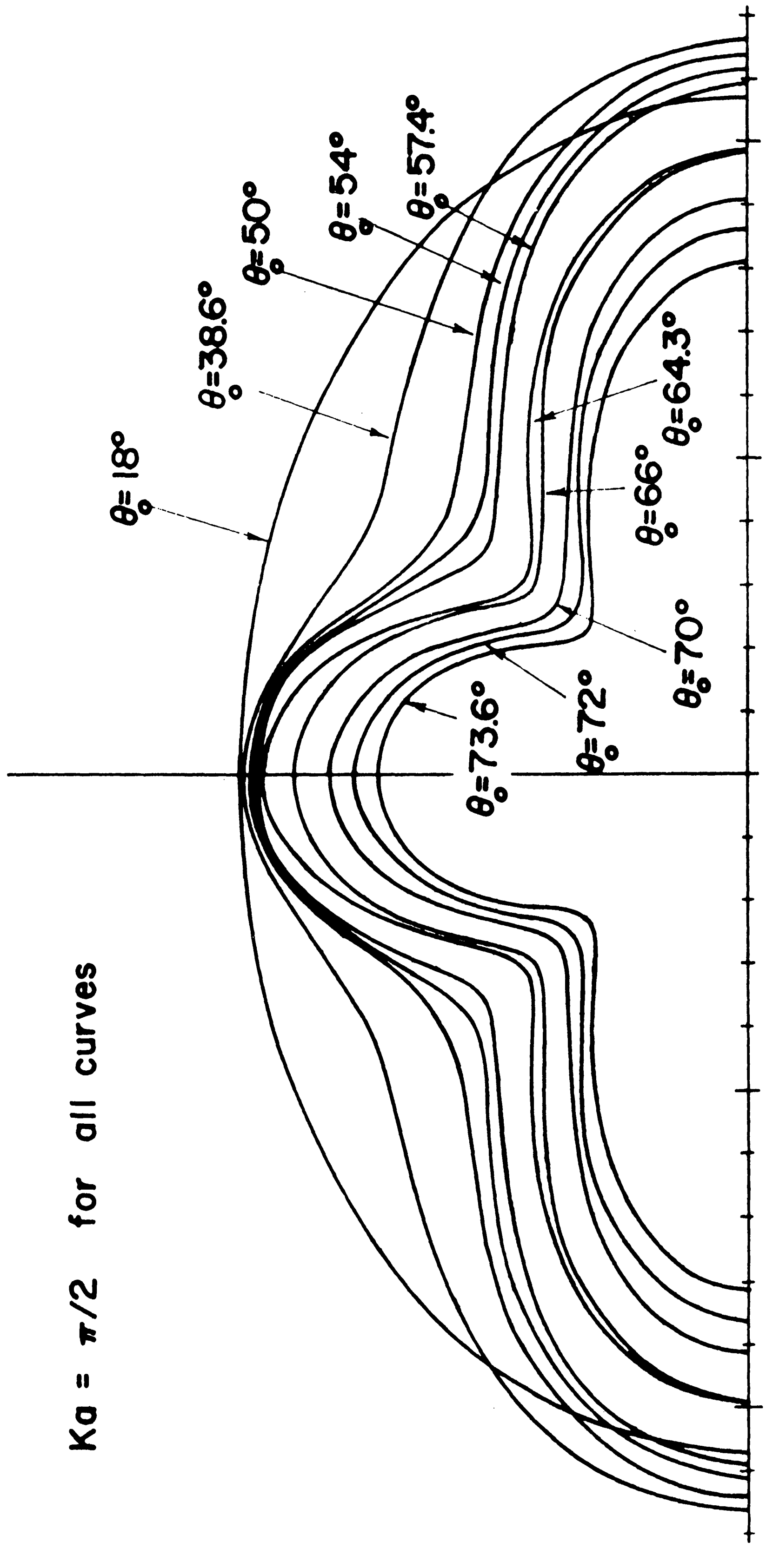

FIGURE 5. RADIATION PATTERNS FOR BI-WEDGES CALCULATED BY TRUNCATING THE INFINITE MATRIX AND INVERTING IT

degrees. Judging from a comparison of Figures 3, 4 and 5 the thin bi-wedge expressions should give useable results for wedge angles as large as $\theta_o = 20^o$ and the thick bi-wedge expressions should be useable for wedge angles as small as $\theta_o = 54^o$. Further proof of this can be given by constructing a table for radiation pattern points, comparing values obtained from the inverted matrix for $\theta_o = 18^o$, $ka = \frac{\pi}{2}$ to values obtained when the thin bi-wedge formulas are used for $\theta_o = 18^o$ and $ka = \frac{\pi}{2}$, and from the inverted matrix for $\theta_o = 73.6^o$, $ka = \frac{\pi}{2}$ to values obtained when the thick bi-wedge expressions are used for the same parameters. To make comparison easy the $\theta = 0^o$ values are normalized to the value one.

	Thin	Matrix	Matrix	Thick
θ \ θ_o	18^o	18^o	74.6^o	74.6^o
0^o	1.0	1.0	1.0	1.0
10^o	.996	.992	.953	.949
20^o	.983	.972	.824	.815
30^o	.964	.940	.649	.627
40^o	.940	.901	.491	.480
50^o	.916	.860	.443	.416
60^o	.894	.824	.519	.510
70^o	.878	.799	.632	.625
80^o	.869	.785	.718	.747
90^o	.866	.781	.749	.792

BIBLIOGRAPHY
(for Appendix C)

1. Bateman Manuscript Project, Higher Transcendental Functions, Vol. I, McGraw-Hill Book Co., 1953.

2. Davis, H. T., Tables of the Higher Mathematical Functions, Vol. I and II, The Principia Press, Inc., Bloomington, Indiana, 1933 and 1935.

3. Knopp, K., Theory and Application of Infinite Series, Hafner Publishing Company, New York, 1928.

BIBLIOGRAPHY

1. Schelkunoff, S. A., "Theory of Antennas of Arbitrary Size and Shape", Proceedings of the IRE, 29, (493) (September 1941).

2. Papas, C. H. and King, R., "Input Impedance of Wide-Angle Conical Antennas", Cruft Laboratory, Harvard University, Cambridge, Mass. (December 1, 1948).

3. Smith, P. D. P., "The Conical Dipole of Wide Angle", Journal of Applied Physics, 19, (11) (January 1948).

4. Tai, C. T., "Application of a Variational Principle to Biconical Antennas", Journal of Applied Physics, 20, (1076), (November 1949).

5. Robin, L. and Pereira-Gomes, A., "L'Antenne Biconique, Symetrique, D'Angle Quelconque", Annales des Telecommunications, 8, (382) (1953).

6. Schelkunoff, S. A., Advanced Antenna Theory, John Wiley and Sons, Inc., New York, (1952).

7. Hobson, E. W., The Theory of Spherical and Ellipsoidal Harmonics, Cambridge University Press, Cambridge, (1956).

8. Knopp, K., Theory and Application of Infinite Series, Hafner Publishing Company, New York, (1928).

9. Kontorvich, L. V. and Krylov, V. I., Approximate Methods of Higher Analysis, Interscience Publishers, Inc., New York, (1958).

10. Schelkunoff, S. A., "General Theory of Symmetric Biconical Antennas", Journal of Applied Physics, 22, (1330) (November 1951).

11. Meier, J. A., and Leitner, A., Biconical Antenna, Interim Technical Report No. 6, Department of Mathematics and Physics, Michigan State University, (June 1957).

12. Tallqvist, H. J., Sechsstellige Tafeln der 32 ersten Kugelfunktionen $P_n(\cos\theta)$ Acta Soc. Sci. Fennicae, Vol. 11 (2) (1938).